© 2019. Published by The Company of Biologists Ltd | Journal of Cell Science (2019) 132, jcs232157. doi:10.1242/jcs.232157

RESEARCH ARTICLE

Cross-talk between TGF-β and PDGFRα signaling pathways regulates the fate of stromal fibro–adipogenic progenitors

Osvaldo Contreras[1,2,*], Meilyn Cruz-Soca[1], Marine Theret[2], Hesham Soliman[2,3], Lin Wei Tung[2], Elena Groppa[2], Fabio M. Rossi[2] and Enrique Brandan[1,*]

ABSTRACT

Fibro–adipogenic progenitors (FAPs) are tissue-resident mesenchymal stromal cells (MSCs) required for proper skeletal muscle development, regeneration and maintenance. However, FAPs are also responsible for fibro-fatty scar deposition following chronic damage. We aimed to investigate the role of functional cross-talk between TGF-β and PDGFRα signaling pathways in the fate of FAPs. Here, we show that the number of FAPs correlates with TGF-β levels and with extracellular matrix deposition during regeneration and repair. Interestingly, the expression of PDGFRα changed dynamically in the fibroblast lineage after injury. Furthermore, PDGFRα-dependent immediate early gene expression changed during regeneration and repair. We also found that TGF-β signaling reduces PDGFRα expression in FAPs, mouse dermal fibroblasts and in two related mesenchymal cell lines. Moreover, TGF-β promotes myofibroblast differentiation of FAPs but inhibits their adipogenicity. Accordingly, TGF-β impairs the expression of PDGFRα-dependent immediate early genes in a TGFBR1-dependent manner. Finally, pharmacological inhibition of PDGFRα activity with AG1296 impaired TGF-β-induced extracellular matrix remodeling, Smad2 signaling, myofibroblast differentiation and migration of MSCs. Thus, our work establishes a functional cross-talk between TGF-β and PDGFRα signaling pathways that is involved in regulating the biology of FAPs and/or MSCs.

This article has an associated First Person interview with the first author of the paper.

KEY WORDS: Regeneration, Fibrosis, Myofibroblast, Mesenchymal progenitors, Fibroblast, Skeletal muscle

INTRODUCTION

Adult skeletal muscle has a remarkable regeneration capacity following injury, making this an attractive tissue model to study regeneration and repair. Muscle stem cells (MuSCs), also known as satellite cells, are essential in these processes (Lepper et al., 2011; Murphy et al., 2011; Sambasivan et al., 2011). A different population of interstitial tissue-resident mesenchymal stromal cells (MSCs), called fibro-adipogenic progenitors (FAPs), is also necessary for effective regeneration and maintenance of skeletal muscle, since it supports MuSC expansion and differentiation *in vitro* and *in vivo* (Heredia et al., 2013; Fiore et al., 2016; Joe et al., 2010; Mathew et al., 2011; Uezumi et al., 2010; Wosczyna et al., 2019). Genetic ablation of PDGFRα$^+$ FAPs results in impaired MuSC and CD45$^+$ hematopoietic cell expansion after injury, and deficient skeletal muscle regeneration. Furthermore, FAPs are required for homeostatic skeletal muscle maintenance (Wosczyna et al., 2019; Lemos and Duffield, 2018). However, MSCs are also the principal drivers of fibrosis and scar formation during failed regeneration following chronic damage.

FAPs express high levels of platelet-derived growth factor receptor α (PDGFRα, also known as PDGFRA) (Joe et al., 2010; Uezumi et al., 2010; Vallecillo-García et al., 2017; Wosczyna et al., 2012), a receptor tyrosine kinase (RTK) for PDGF-A, PDGF-B and PDGF-C. This RTK plays essential roles during development, stemness, migration and proliferation (Hoch and Soriano, 2003). PDGFRα signaling pathway activation via PDGF ligands regulates the proliferation and differentiation of FAPs (Uezumi et al., 2014a). Although PDGFRα signaling activates core RTK effectors such as the Ras, MAP kinase (MAPK) and phosphatidylinositol-3-OH kinase (PI3K) protein families, the signaling specificity of PDGFRα signaling is mediated through multiple immediate early genes (IEG) (Schmahl et al., 2007). Among these PDGFRα transcriptional target genes are *Txnip*, *Tiparp*, *Arid5b*, *Axud1* (also known as *Csrnp1*) and *Schip1* (Chen et al., 2004; Schmahl et al., 2007; Wu et al., 2008).

Stromal PDGFRα$^+$ cells expand in models of acute and chronic skeletal muscle damage (Contreras et al., 2016; Gonzalez et al., 2017; Mueller et al., 2016; Uezumi et al., 2014a, 2011). PDGFRα signaling is chronically overactivated in the murine Duchenne muscular dystrophy (DMD) model (*mdx* mice) and human DMD, compared to the transiently upregulated signaling in acute injury (Ieronimakis et al., 2016). Overexpression of PDGFRα by FAPs that carry constitutively active PDGFRα mutations promotes their activation and muscle fibrosis, negatively affecting skeletal muscle regeneration (Ieronimakis et al., 2016). Furthermore, treatment with crenolanib and nilotinib (two potent PDGFRα inhibitors) reduces FAP activation and fibrosis during chronic muscle damage (Ieronimakis et al., 2016; Lemos et al., 2015). Changes in the polyadenylation pattern of *Pdgfra* during muscle regeneration regulate the biology and fibrogenic behavior of FAPs (Contreras and Brandan, 2017; Mueller et al., 2016). Taken together, these previous findings suggest that modulating PDGFRα signaling in stromal cells *in vivo* and *in vitro* affects their activity, muscle fibrosis and tissue regeneration. Thus, there is a need to understand FAP biology and the role of PDGFRα under damage and fibrotic conditions, as these cells could be a target for the development of new therapies for several pathologies.

Transforming growth factor beta (TGF-β) is the most-studied pro-fibrotic factor involved in tissue fibrosis to date (Ceco and McNally, 2013; Smith and Barton, 2018). Mammals express three different TGF-β isoforms: TGF-β1 (TGFB1), TGF-β2 (TGFB2) and TGF-β3

[1]Departamento de Biología Celular y Molecular and Center for Aging and Regeneration (CARE-ChileUC), Facultad de Ciencias Biológicas, Pontificia Universidad Católica de Chile, 8331150 Santiago, Chile. [2]Biomedical Research Centre, Department of Medical Genetics and School of Biomedical Engineering, University of British Columbia, V6T 1Z3 Vancouver, BC, Canada. [3]Faculty of Pharmacy, Minia University, 61519 Minia, Egypt.

*Authors for correspondence (oicontre@uc.cl; ebrandan@bio.puc.cl)

O.C., 0000-0002-8722-9371; F.M.R., 0000-0002-0368-2620; E.B., 0000-0002-6820-5059

Received 21 March 2019; Accepted 12 August 2019

Journal of Cell Science (2019) 132, jcs232157. doi:10.1242/jcs.232157

(TGFB3). Expression of the three TGF-β isoforms and TGF-β signaling are upregulated in DMD patients (Bernasconi et al., 1999; Smith and Barton, 2018) and in skeletal muscles of the *mdx* mouse (Acuña et al., 2014; Gosselin et al., 2004; Lemos et al., 2015), therefore participating in tissue fibrosis in several organs (Kim et al., 2018). Overactivated TGF-β signaling correlates with increased fibrosis but reduced angiogenesis, tissue function and muscle regeneration (Juban et al., 2018; Mann et al., 2011; Pessina et al., 2015; Vidal et al., 2008). Interestingly, TGF-β inhibition improves the pathophysiology of muscular dystrophies (Accornero et al., 2014; Acuña et al., 2014; Ceco and McNally, 2013; Cohn et al., 2007; Danna et al., 2014). The three TGF-β isoforms stimulate FAP proliferation, ECM production and myofibroblast differentiation (Lemos et al., 2015; Uezumi et al., 2011). Macrophages and FAPs appear to be the major sources of TGF-β in damaged muscle (Juban et al., 2018; Lemos et al., 2015; Pessina et al., 2015). After TGF-β binding to the heteromeric serine-threonine kinase receptors TGFBR1 (also known as ALK5), TGFBR2 and TGFBR3 on the cell surface, the Smad tri-complex (Smad2–Smad3–Smad4) translocates to the nucleus, where it recognizes Smad-binding elements (SBE) on its target genes (Hinz et al., 2007; Kim et al., 2018; David and Massagué, 2018). TGF-β also acts via non-canonical pathways, such as p38 MAPK, ERK1/2, PI3K and JNK (Derynck and Zhang, 2003). These pathways, along with canonical TGF-β signaling, are involved in myofibroblast activation and fibrogenesis (Kim et al., 2018). Hence, understanding the role of TGF-β signaling in MSCs is of great importance for the development of effective anti-fibrotic strategies and to improve tissue function. Given that TGF-β and PDGFRα signaling are two of the main pathways governing connective tissue biology, myofibroblast differentiation and ECM remodeling in several organs, exploring their cross-modulation could reveal novel points of therapeutic intervention (Smith and Barton, 2018).

Here, we investigated FAP behavior during skeletal muscle regeneration and repair, as well as the effects of TGF-β signaling on PDGFRα expression. Furthermore, we also studied the role of PDGFRα in TGF-β-mediated responses in mesenchymal progenitors. AG1296 pharmacological inhibition of PDGFRα kinase activity suggested that PDGFRα has a pivotal role in TGF-β-mediated biological responses.

RESULTS

FAPs are dynamically associated with TGF-β levels and fibrosis during regeneration and repair

We used PDGFRα^{H2BEGFP} knock-in reporter mice (Hamilton et al., 2003) to determine FAP numbers and behavior (Lemos et al., 2015). These cells were identified by the PDGFRα-dependent expression of a nuclear-localized fusion protein between histone H2B and EGFP, after acute and chronic skeletal muscle damage in three distinct muscle injury models with different regeneration/repair kinetics (Fig. 1A; Fig. S1). We also determined how FAP fate correlates with TGF-β levels and the degree of fibrosis *in vivo* (Fig. S1). Acute muscle damage with glycerol increased FAP number transiently (Fig. S1A,B) (Kopinke et al., 2017; Uezumi et al., 2010). Increased TGF-β1 mRNA levels and fibrosis follow a similar kinetics pattern as the number of FAPs (Fig. S1C,D) (Ieronimakis et al., 2016). Moreover, FAP number doubles 2 weeks after denervation (Fig. S1E,F). TGF-β1 mRNA also increases after denervation (Fig. S1G). Using wheat germ agglutinin (WGA) and picrosirius staining, we observed increases in muscle atrophy and mild fibrosis after denervation (Fig. S1E,H) (Contreras et al., 2016; Madaro et al., 2018; Rebolledo et al., 2019). Finally, we evaluated the number of FAPs in adult (5-month-old) *mdx* mice (*mdx*; PDGFRα^{H2BEGFP}) (Fig. S1I). FAP numbers expanded 2.5-fold in *mdx*;PDGFRα^{H2BEGFP} diaphragm muscle compared with non-dystrophic PDGFRα^{H2BEGFP} mice (Fig. S1J) (Contreras et al., 2016). Concurrently, augmented and sustained TGF-β expression and fibrosis were also observed in the adult *mdx* diaphragm (Fig. S1K–N) (Acuña et al., 2014; Pessina et al., 2015). Moreover, we found a positive correlation between FAP expansion, TGF-β levels and total collagen following injury (Fig. S1L). Thus, our results suggest that the expansion of resident FAPs is closely associated with elevated pro-fibrotic TGF-β levels and increased fibrosis during regeneration and repair.

Dynamics of PDGFRα expression in stromal PDGFRα$^{H2BEGFP+}$ cells during regeneration and repair

To study whether the expression of PDGFRα in FAPs changes during regeneration and repair, we used the muscle injury models presented above. Intriguingly, we found changes in PDGFRα expression after acute damage with glycerol at day 3 and day 7, where the proportion of EGFP^{+} cells expressing low levels of PDGFRα (PDGFRα–EGFP$^{medium/low}$) was larger compared to undamaged muscle. In the latter case, PDGFRα expression was generally high (PDGFRα–EGFP^{high}) (Fig. S1A). To further explore our initial observation, we took advantage of confocal microscopy using *z*-stack reconstructions of 7-µm-thick transverse sections and analyzed the percentage of PDGFRα–EGFP$^{medium/low}$-expressing FAPs in regeneration and repair (Fig. 1A–C). PDGFRα–EGFP^{high} FAPs were distributed throughout the muscle interstitium as labeled using collagen type 1, consistent with previous studies of FAP distribution (Fig. 1A) (Lemos et al., 2015; Uezumi et al., 2010). In PDGFRα^{H2BEGFP} muscles 7-days-post-glycerol damage and in the dystrophic diaphragm, we found accumulation of PDGFRα–EGFP$^{medium/low}$-expressing FAPs corresponding to ECM-enriched areas (Fig. 1A–C). PDGFRα–EGFP$^{medium/low}$ cells were found to expand according to the extension of tissue inflammation, damage and fibrosis, and hence they were abundant in the inflammatory glycerol-damaged and dystrophic models (Fig. 1A,C; Fig. S1). However, we did not detect significant changes in PDGFRα expression in the EGFP^{+} population using the mild-inflammatory model of muscle denervation (Fig. 1A,C).

We further corroborated our results using *in vivo* flow cytometry analyses of undamaged muscles expressing PDGFRα^{H2BEGFP}, *mdx* dystrophic muscle and fibrotic-*mdx* muscle (see Materials and Methods section for details) (Fig. 1D). In undamaged muscles virtually all EGFP^{+} FAPs were PDGFRα–EGFP^{high} (Fig. 1D), but neither MuSCs (α7-integrin^{+}), hematopoietic (CD45^{+}) nor endothelial (CD31^{+}) cells showed detectable EGFP (Fig. 1D). Adult *mdx* TA muscle showed small accumulations of PDGFRα–EGFP$^{medium/low}$ cells, which increased in fibrotic *mdx* TA muscle (Fig. 1D). These results suggest that different FAP sub-populations (expressing different levels of PDGFRα) take part in the regenerative process after damage (Malecova et al., 2018). We also speculate that damage-associated signaling might regulate FAP PDGFRα expression and function endogenously during tissue repair. Single-cell RNA sequencing analysis (scRNAseq) from recent work on cardiac damage helped us to corroborate our hypothesis (Farbehi et al., 2019). Two major clusters of EGFP^{+} cells are identified in which PDGFRα–EGFP$^{medium/low}$ cells expressed elevated levels of differentiation marker transcripts such as *Tgfb1*, the matricellular protein connective tissue growth factor *Ccn2* (also known as *Ctgf*), and *Col1a1* (Fig. 1E). A negative correlation between the expression of PDGFRα and TGF-β ligands was found in stromal fibroblasts and periostin^{+} myofibroblasts after myocardial infarction (Fig. 1F; Fig. S2). Taken together, these results suggest that stromal PDGFRα^{+} cells are heterogeneous and dynamic in injured adult tissues where the myofibroblast populations could be distinguished by the repression of PDGFRα.

Journal of Cell Science (2019) 132, jcs232157. doi:10.1242/jcs.232157

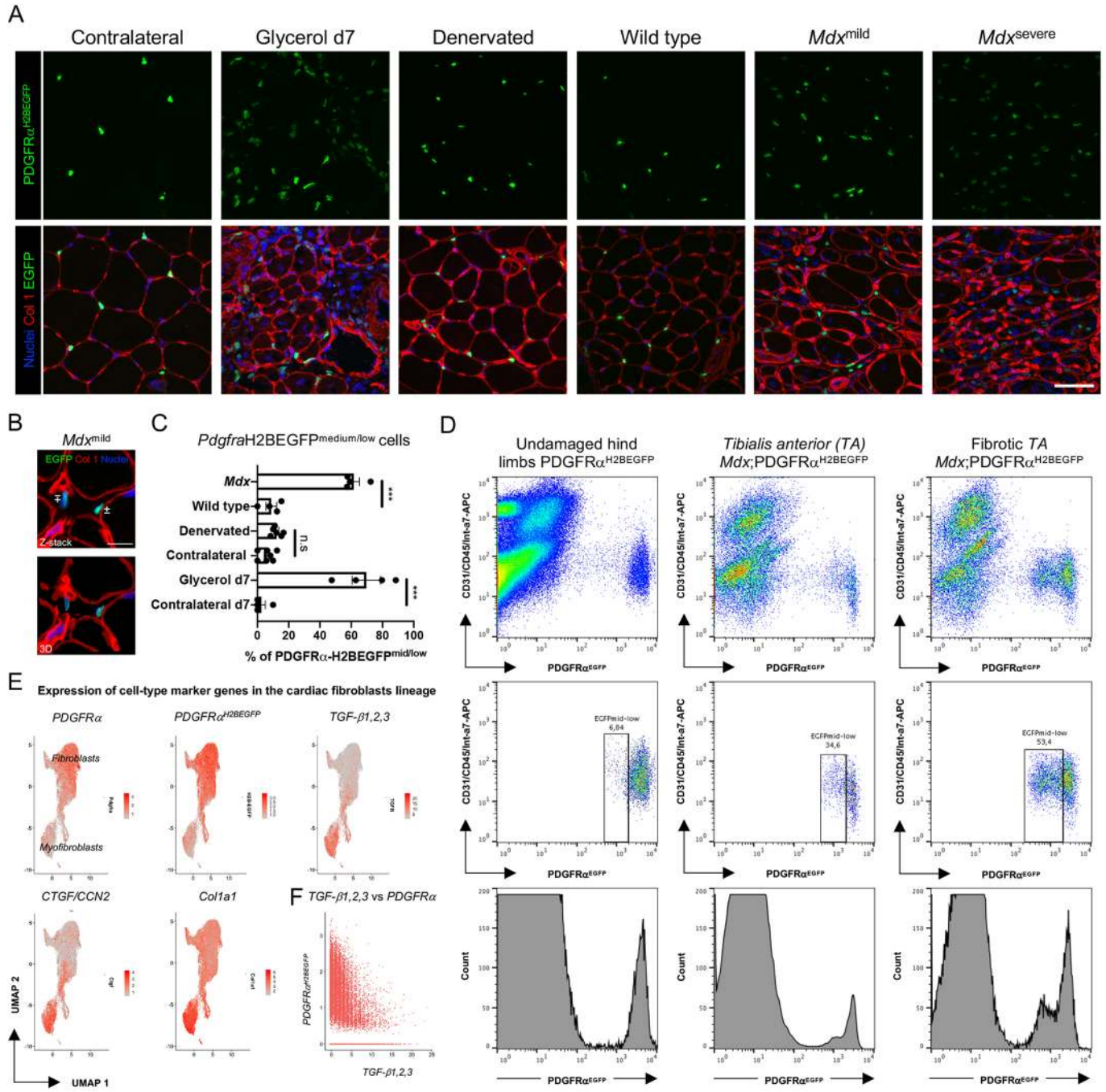

Fig. 1. Dynamics of PDGFRα expression in PDGFRα$^{H2BEGFP+}$ FAPs during regeneration and repair. (A) *Z*-stack confocal images showing the localization of PDGFRα–EGFP^{+} cells in skeletal muscle sections of adult PDGFRα$^{H2BEGFP/+}$ knock-in mice under different injury and damage models: tibialis anterior glycerol day 7, gastrocnemius 2 weeks of denervation, and diaphragm from the dystrophic *mdx* background. Scale bar: 50 µm. (B) *Z*-stack (top) and 3D alpha blend reconstruction (bottom) showing two single PDGFRα-expressing cells, PDGFRα–EGFP^{high} (±) and PDGFRα–EGFP$^{medium/low}$ (∓) in a diaphragm section of *mdx*^{mild}. (C) Quantification of the percentage of PDGFRα–EGFP$^{medium/low}$ cells in the different damage models. ***P<0.001; n.s., not significant by two-tailed Student's *t*-test. Wild-type, *mdx*, glycerol day 7 and contralateral day 7; n=4. Contralateral and denervated; n=6. (D) Flow cytometry analyses of CD31/CD45/α7-integrin–APC (negative) and PDGFRα–EGFP (positive) cells from PDGFRα^{H2BEGFP} and *mdx*;PDGFRα^{H2BEGFP} mice, displaying the reduced EGFP expression in FAPs according to the extension of damage in dystrophic *mdx* TA muscle. (E) Single-cell RNA sequencing analyses showing the expression of a subset of cell-state marker genes in the cardiac fibroblast PDGFRα$^{H2BEGFP/+}$ lineage, using the uniform manifold approximation and projection (UMAP) algorithm (McInnes et al., 2018). (F) The negative correlation between TGF-β ligands (TGF-β1, TGF-β2 and TGF-β3) expression and PDGFRα expression in the cardiac PDGFRα^{EGFP+} stromal lineage is shown.

PDGFRα immediate early gene expression varies during skeletal muscle regeneration, denervation, and in dystrophic *mdx* mice

Muscle injury induces FAP activation, proliferation and differentiation (Lemos et al., 2015; Uezumi et al., 2010). Likewise, we previously reported that PDGFRα IEG expression changed in skeletal muscle of symptomatic hSOD1^{G93A} mice [amyotrophic lateral sclerosis (ALS) mouse model], where upregulated TGF-β levels, FAP cells and ECM deposition were found (Gonzalez et al., 2017; Madaro et al., 2018). Thus, we used the skeletal muscle models

presented above to evaluate the PDGFRα IEG response to FAP activation and muscle damage. We decided to evaluate the expression of PDGFRα target genes after 3 and 7 days of glycerol injection as FAP expansion peaks at this time and the PDGFRα–EGFP$^{medium/low}$ population appears in the EGFP^{+} population (Fig. S1A,B) (Kopinke et al., 2017). Glycerol acute damage altered the expression of the evaluated PDGFRα IEG (Fig. 2A,B). *Txnip*, *Tiparp* and *Schip1* expression was repressed, but *Arid5b* expression increased threefold (Fig. 2A,B). Importantly, *in silico* manual search of microarray data generated from a different study further corroborated *Txnip* repression during regeneration (Table S1) (Lukjanenko et al., 2013).

Since FAP activation and ECM remodeling start early during skeletal muscle denervation (Contreras et al., 2016; Rebolledo et al., 2019), we decided to evaluate PDGFRα IEG expression at day 4 (early) and at day 14 (late) post-denervation. *Txnip* expression was repressed by 90%, while *Axud1* and *Ship1* expression was increased after early denervation (Fig. 2C). Similarly, 14 days of denervation significantly reduced *Txnip* expression and increased *Ship1* expression (Fig. 2D). However, contrary to what we observed on day 4, *Axud1* expression decreased 14 days after denervation. Finally, we tested whether the PDGFRα-dependent signaling pathway was also impaired in old dystrophic *mdx* muscles. We found that *Txnip*, *Arid5b*, *Tiparp*, *Axud1* and *Schip1* were downregulated in the fibrotic gastrocnemius and diaphragm muscles of old *mdx* mice when compared to wild-type mice (Fig. 2E,F). Taken together, our results show that the expression of PDGFRα IEG varies depending on the model of muscle damage and regeneration used.

TGF-β signaling downregulates PDGFRα expression in fibro-adipogenic progenitors and mesenchymal stromal cell lines

Our previous results indicate that damage and TGF-β-induced fibrogenic state negatively correlate with PDGFRα expression in FAPs. Therefore, we investigated the role of TGF-β signaling on PDGFRα expression in FAPs. Table 1 shows different putative transcription factor binding sites associated with TGF-β signaling in the mouse PDGFRα promoter, which we found to be highly enriched for GC-box SP1 factors, and also to contain one SBE site (GTCT), and two activating protein 1 (AP1) sites (A/TTCA) (Zhang, 2017). These findings suggest that PDGFRα could be a direct target of TGF-β signaling. Furthermore, BioGRID-based human PDGFRα interaction network analysis shows that PDGFRα interacts with the TGF-β receptor type-2 (TGFBR2) (Fig. S3A). Importantly, the three TGF-β isoforms and TGF-β receptors are expressed in FAPs and MSCs at the mRNA and protein levels (Fig. S3B–D). Thus, we isolated EGFP^{+} FAPs from undamaged limb muscles using FACS and treated them with pathophysiological amounts of TGF-β1 (Fig. 3A,B). When EGFP^{+} FAPs were treated with TGF-β1, PDGFRα expression diminished dramatically, with its protein levels becoming almost undetectable at 24 h (∼90% reduction) (Fig. 3B,C). We corroborated these results with limb and diaphragm wild-type FAPs (Fig. 3D,E). Treatment with TGF-β1 also increases the expression of matricellular CCN2 and αSMA (myofibroblast marker, also known as ACTA2) proteins in FAPs (Fig. 1C,D) (Uezumi et al., 2011). Since we observed that TGF-β downregulated PDGFRα in skeletal muscle FAPs, we verified whether it similarly affects cardiac FAPs from PDGFRα^{H2BEGFP} mice (Fig. S4A,B). TGF-β1 was also observed to reduce PDGFRα protein expression in EGFP^{+} cardiac FAPs, although to a lesser extent than skeletal muscle FAPs (Fig. S4C). Taken together, these results demonstrate that TGF-β signaling downregulates the expression of the MSC and fibroblast pan-marker PDGFRα in tissue-resident progenitors.

The multipotent cell line C3H/10T1/2 is widely used to study mesenchymal progenitor fate and fibroblast-related behavior (Braun et al., 1989; Reznikoff et al., 1973; Singh et al., 2003). Thus, we decided to use these cells as a complementary *in vitro* model of MSCs to corroborate our previous results. Consistent with the results presented above, TGF-β1 stimulation also diminished PDGFRα expression in C3H/10T1/2 cells at 8 h and 24 h of treatment (Fig. 3F). Membrane and cytoplasmic PDGFRα staining in C3H/10T1/2 MSCs was reduced in response to TGF-β (Fig. S4D–F). Next, we used another established fibroblast cell line (NIH-3T3), to further validate our results. Indeed, TGF-β1 also repressed PDGFRα expression in these cells at concentrations of 0.5 ng/ml and higher (Fig. 3G). As expected, CCN2 and αSMA proteins increased in these two cell lines after TGF-β1 treatment, since this pro-fibrotic cytokine is known to

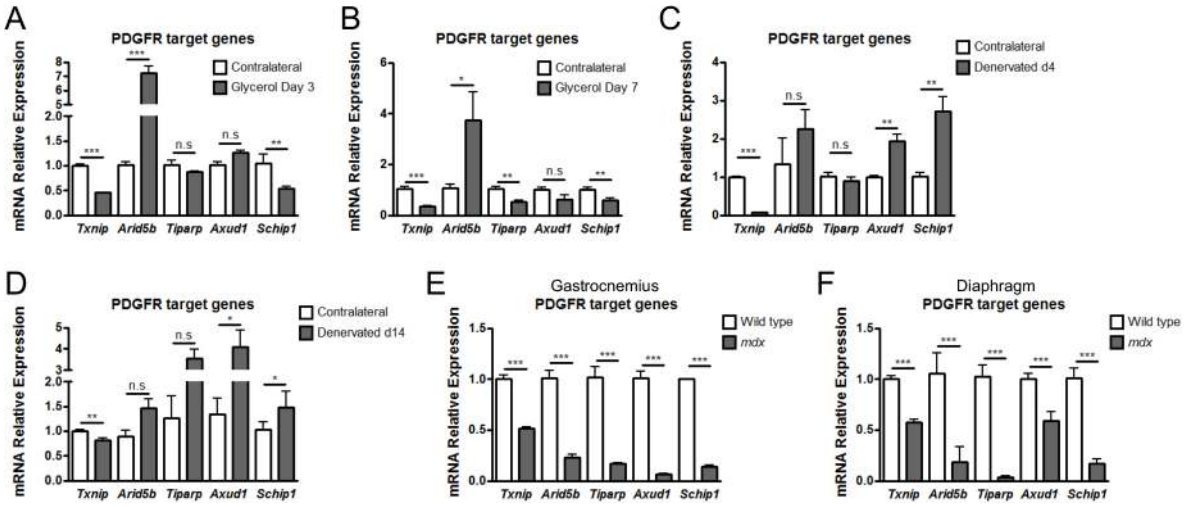

Fig. 2. The expression of PDGFRα-dependent immediate early genes varies during skeletal muscle regeneration, denervation and muscular dystrophy. (A,B) Skeletal muscle *Txnip*, *Arid5b*, *Tiparp*, *Axud1* and *Schip1* mRNA expression was analyzed by quantitative PCR at 3 days (A) and 7 days (B) after acute glycerol TA damage. ***P<0.001; **P<0.005; *P<0.05; n.s., not significant by two-tailed Student's t-test; n=3. (C,D) PDGFRα IEG expression levels were analyzed by quantitative PCR at early (4 days) (C) and late (14 days) (D) stages in gastrocnemius muscle after sciatic denervation. (E,F) PDGFRα IEG expression was analyzed by quantitative PCR in gastrocnemius (E) and diaphragm (F) muscles from 24-month-old wild-type and *mdx* mice.

Journal of Cell Science (2019) 132, jcs232157. doi:10.1242/jcs.232157

Table 1. Transcription factor-binding sites linked to TGF-β signaling in the PDGFRα promoter

Number	Family	Matrix	Detailed family information	Start (bp)	End (bp)	Strand	Matrix sim.	Core sim.	Sequence
38	V$SP1F	V$TIEG.01	GC-Box factors SP1/GC	96	112	–	0.934	1	ggggGGGGtgtgagaag
42	V$SP1F	V$TIEG.01	GC-Box factors SP1/GC	98	114	–	0.916	1	ggggGGGGggtgtgaga
54	V$SP1F	V$GC.01	GC-Box factors SP1/GC	102	118	–	0.907	0.819	tgtgggGGGGggggtgt
65	V$SP1F	V$TIEG.01	GC-Box factors SP1/GC	116	132	–	0.879	0.75	ttttGGTGtgtgtgtgt
76	V$SP1F	V$SP2.01	GC-Box factors SP1/GC	157	173	–	0.801	0.772	gggaagggagGGCCttc
99	V$SP1F	V$SP2.01	GC-Box factors SP1/GC	187	203	–	0.847	1	gggcgaagcgGGACttc
173	V$SP1F	V$SP2.01	GC-Box factors SP1/GC	485	501	+	0.83	1	aacaaaggcaGGACcag
258	V$SMAD	V$SMAD3.01	Vertebrate SMAD family of transcription factors	756	766	–	0.994	1	acaGTCTgggc
297	V$SP1F	V$GC.01	GC-Box factors SP1/GC	865	881	–	0.922	0.872	tttgggGGTGggggtgc
331	V$SP1F	V$GC.01	GC-Box factors SP1/GC	952	968	–	0.89	0.877	gaagggGGAGgtgttga
347	V$SP1F	V$GC.01	GC-Box factors SP1/GC	969	985	–	0.881	0.872	gggtggGGTGgggggcc
355	V$SP1F	V$GC.01	GC-Box factors SP1/GC	974	990	–	0.913	0.872	agatggGGTGgggtggg
416	V$SP1F	V$SP1.01	GC-Box factors SP1/GC	1140	1156	+	0.896	0.772	caaggGGGGgggggact
416	V$SP1F	V$SP1.01	GC-Box factors SP1/GC	1140	1156	+	0.896	0.772	caaggGGGGgggggact
462	V$AP1F	V$BATF.01	AP1, Activating protein 1	1217	1229	+	0.929	0.818	cattgaATCAatt
463	V$AP1F	V$BATF.01	AP1, Activating protein 1	1217	1229	–	0.951	0.888	aattgaTTCAatg

Putative transcription factor-binding sites (TFBS) linked to TGF-β signaling in the mouse PDGFRα promoter are shown. The analysis was performed using MatInspector (https://www.genomatix.de/online_help/help_matinspector/matinspector_help.html). In the nucleotide sequence, capital letters correspond to the core sequence and lower-case letters indicate a high conservation value in the matrix. Each position is relative to the initiation of transcription.

induce myofibroblast differentiation of both MSC and fibroblast cell lines (Fig. 3F,G) (Gutiérrez et al., 2015; Riquelme-Guzmán et al., 2018). Finally, to elucidate whether the described PDGFRα downregulation might also occur in MSCs and fibroblasts originating from a different tissue, we cultured primary mouse dermal fibroblasts (MDFs) isolated from the skin. TGF-β1 treatment also reduced PDGFRα levels in MDFs along with the induction of CCN2 protein (Fig. S4G). Since TGF-β signaling in mammals is also activated by TGF-β2 and TGF-β3, we evaluated whether these cytokines influence PDGFRα expression in MSCs. Both TGF-β2 and TGF-β3 strongly reduced PDGFRα expression in MSCs (Fig. S4H). Quantitative analysis showed a 90% decrease in PDGFRα expression after a 24 h stimulation with both cytokines (Fig. S4I), similar to the effects observed for TGF-β1. Thus, the three TGF-β cytokines reduce PDGFRα expression in mesenchymal stromal cells. Interestingly, TGF-β not only diminishes PDGFRα expression but also influences its own signaling by downregulating TGFBR2 protein expression in MSCs (Fig. S4J). Overall, these results indicate that, along with inducing myofibroblast differentiation, TGF-β also inhibits the expression of PDGFRα in skeletal muscle and cardiac FAPs, MDFs, and in two different mesenchymal cell lines, C3H/10T1/2 and NIH-3T3.

As shown above, we demonstrated that TGF-β represses the expression of PDGFRα during the fibroblast-to-myofibroblast transition. Hence, we asked whether TGF-β signaling could affect FAP differentiation to adipocytes while promoting myofibroblast cell commitment. TGF-β1 stimulation impairs basal FAP differentiation into the adipogenic lineage, therefore reducing the steady-state percentage of perilipin^{+}-adipocytes after 24 h (Fig. 3H–J) but increasing the number of αSMA^{+} cells (myofibroblasts) (Fig. 3J). Moreover, *peroxisome proliferator-activated receptor gamma* (*Pparg*) and *adiponectin* (*Adipoq*) gene expression was reduced by TGF-β treatment in growing FAPs (Fig. 3K). Finally, we also found that PDGFRα expression was repressed after adipogenic differentiation of FAPs and C3H/10T1/2 MSCs (Fig. 3M,N). Thus, TGF-β restricts FAP progression into the adipogenic lineage and FAP-induced adipogenesis downregulates PDGFRα expression. These data suggest that the transcriptional regulation of myofibroblast differentiation is directly connected to the adipogenic potential of FAP cells.

TGF-β-mediated PDGFRα downregulation requires TGF-β receptor type-I and the p38 MAPK signaling pathway

To investigate the role of TGF-β receptors in the regulation of PDGFRα by TGF-β, we used SB525334, a specific small-molecule inhibitor of TGFBR1 (Callahan et al., 2002). SB525334 blocks the ATP-binding site of TGFBR1 and inhibits TGF-β–induced TGFBR1 serine/threonine kinase activity, thereby preventing phosphorylation of the Smad complex and the non-canonical pathways along with subsequent gene expression (Laping et al., 2007). Incubation with the TGFBR1 inhibitor completely abolished the effect of TGF-β1 on PDGFRα expression in wild-type FAPs (Fig. 4A). Several SP1 binding sites are located in the PDGFRα promoter and it has been demonstrated that SP1 is regulated by the p38 MAPK signaling pathway (Table 1) (D'Addario et al., 2002; Ma et al., 2001). To investigate the role of p38 MAPK proteins in the regulation of PDGFRα in TGF-β-stimulated FAPs, we first examined their activation in response to TGF-β. TGF-β1 induces non-canonical p38 activation in FAPs and C3H/10T1/2 cells (Fig. 4B; Fig. S5). The p38 MAPK inhibitor SB203580 partially abolishes the reduction of PDGFRα by TGF-β1 in wild-type FAPs and C3H/10T1/2 MSCs (Fig. 4C,D).

It has been suggested that wild-type and *mdx* FAPs behave differently as a result of changes in their activation status and biology (Malecova et al., 2018; Marinkovic et al., 2019). Therefore, young *mdx* FAPs were isolated and treated with TGFBR1 inhibitor and p38 MAPK inhibitor, along with TGF-β1. Both inhibitors blocked the effects of TGF-β1 on PDGFRα levels in *mdx* FAPs, although *mdx* FAPs express reduced PDGFRα protein levels at basal state (Fig. 4F). Also, we found that p38 inhibition reduces TGF-β1-induced CCN2 expression in both wild-type and *mdx* FAPs (Fig. 4C,E). We performed a time-course analysis with the protein synthesis inhibitor cycloheximide and determined that PDGFRα protein half-life is remarkably short, being approximately 2 h in both FAPs and C3H/10T1/2 MSCs ($T_{1/2}$=2 h) (Fig. S6). Overall, these data suggest the participation of TGF-β receptors and the involvement of the TGF-β non-canonical p38 MAPK signaling pathway in the downregulation of PDGFRα in wild-type, *mdx* FAPs and mesenchymal stromal cell lines.

Journal of Cell Science (2019) 132, jcs232157. doi:10.1242/jcs.232157

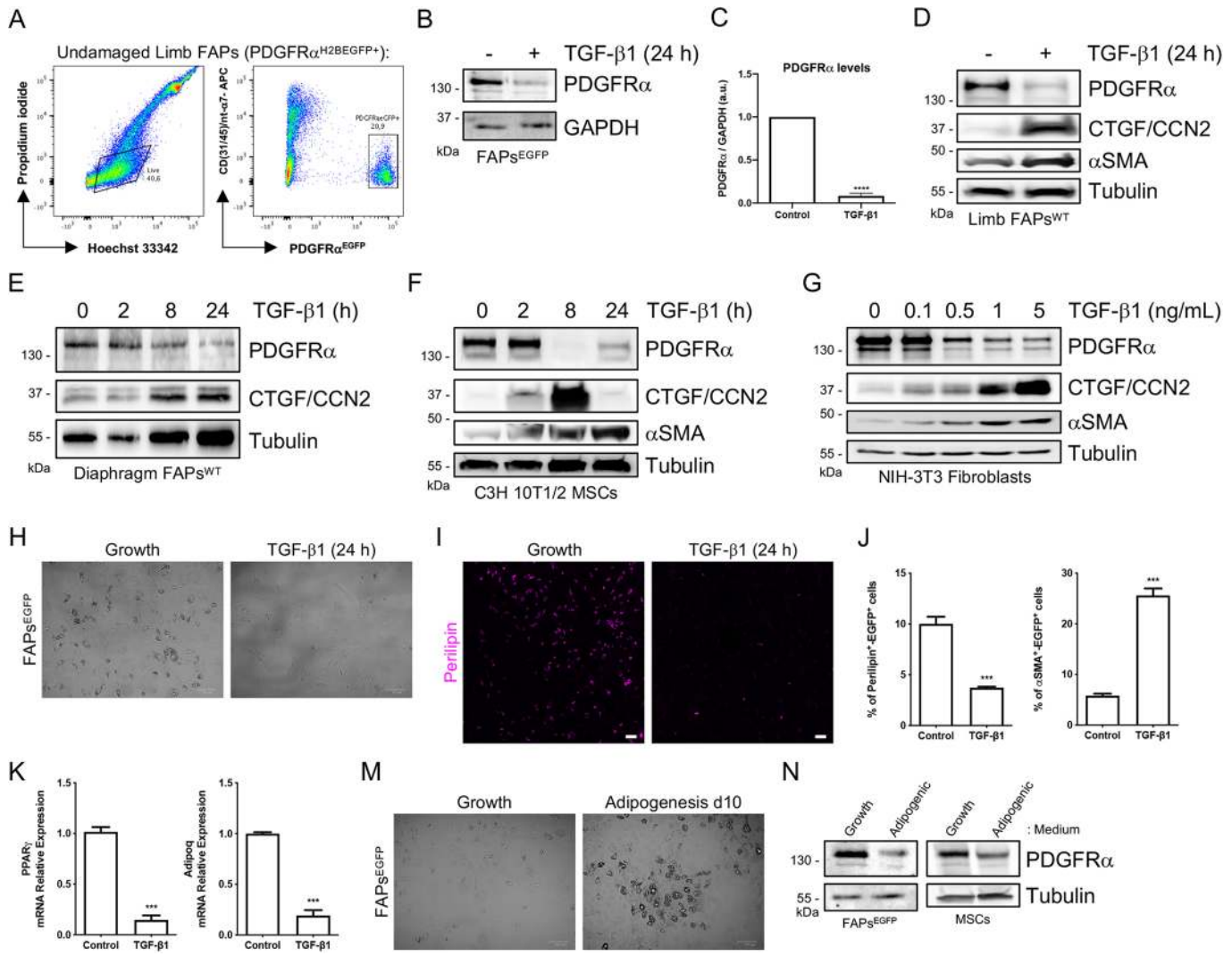

Fig. 3. TGF-β signaling downregulates PDGFRα expression in fibro-adipogenic progenitors and mesenchymal stromal cells. (A) Sequential gating strategy used to isolate adult EGFP$^+$ FAPs from undamaged hindlimb skeletal muscles in samples from reporter PDGFRα$^{H2BEGFP/+}$ knock-in mice. (B) Representative western blot analysis showing PDGFRα expression levels after treatment with 5 ng/ml TGF-β1 (24 h) in EGFP$^+$ FAPs. GAPDH was used as the loading control. (C) Quantification of PDGFRα protein expression. ****P<0.0001 by two-tailed Student's t-test; n=4. (D,E) PDGFRα, CCN2, αSMA and tubulin levels were analyzed by western blot in limb (D) and diaphragm (E) wild-type FAPs treated with TGF-β1 (5 ng/ml). (F) Representative western blot analysis showing PDGFRα, CCN2 and αSMA expression levels in C3H/10T1/2 mesenchymal progenitor cells after treatment with TGF-β1 (5 ng/ml) at different time points (0, 2, 8 and 24 h). Tubulin was used as the loading control. (G) Representative western blot analysis showing PDGFRα, CCN2 and αSMA expression in NIH-3T3 fibroblasts after treatment with different concentrations of TGF-β1 for 24 h. Tubulin was used as the loading control. (H) Bright-field images of skeletal muscle EGFP$^+$ FAPs under growth conditions for 4 days following FACS (left) and then treated with TGF-β1 for 24 h (right). Scale bars: 75 µm. (I) Perilipin immunofluorescence in control and TGF-β1-treated (5 ng/ml, 24 h) EGFP$^+$ FAPs. Scale bar: 100 µm. (J) Quantification of the percentage of perilipin$^+$–EGFP$^+$ and αSMA$^+$–EGFP$^+$ cells in control and TGF-β1-treated (5 ng/ml, 24 h) EGFP$^+$ FAPs. (K) *Pparg* and *Adiponectin* mRNA expression levels were analyzed by quantitative PCR in control and TGF-β1-treated (5 ng/ml, 24 h) wild-type FAPs. ***P<0.001 by two-tailed Student's t-test; n=3. (M) Bright-field images of skeletal muscle EGFP$^+$ FAPs under growing conditions for 4 days following FACS (left), and then adipogenesis induction (10 days) (right). Scale bars: 100 µm. (N) Representative western blot analysis showing PDGFRα expression levels after adipogenesis induction of EGFP$^+$ FAPs (10 days) and C3H 10T1/2 (21 days) mesenchymal progenitors. Tubulin was used as the loading control.

PDGFRα immediate early gene expression is altered by TGF-β signaling in a TGF-β receptor type-I-dependent manner

IEG expression triggered by the PDGFRα signaling pathway mediates *in vivo* and *in vitro* PDGF responses (Chen et al., 2004; Schmahl et al., 2007). To investigate PDGFRα IEG regulation by TGF-β, we evaluated the expression of a set of PDGFRα target genes in MSCs and assessed whether they are responsive to TGF-β. C3H/10T1/2 cells express several PDGFRα IEGs such as *Txnip*, *Axud1*, *Schip1*, *Tiparp* and *Arid5b* (Fig. 5A) (Chen et al., 2004; Schmahl et al., 2007; Wu et al., 2008). Fig. 5B shows that TGF-β1 alters the expression of these genes in C3H/10T1/2 cells. *Txnip* expression is dramatically reduced, whereas *Axud1* and *Schip1* are increased after TGF-β1 treatment as determined by quantitative PCR (Fig. 5B). Interestingly, the effect of TGF-β1 is observed early after 4 h of treatment, peaking 8 h post-treatment (Fig. 5B). Taken together, we found that TGF-β1 stimulation changes the expression of PDGFRα-dependent IEG in MSCs, suggesting that TGF-β influences the PDGFRα-dependent pathway in these cells.

Next, we analyzed the direct role of the serine/threonine kinase activity of TGFBR1 on the expression of PDGFRα IEG *in vitro*. We harvested C3H/10T1/2 cell samples 8 h after TGF-β1 stimulation, as this is the time when we observed the largest changes in PDGFR

Journal of Cell Science (2019) 132, jcs232157. doi:10.1242/jcs.232157

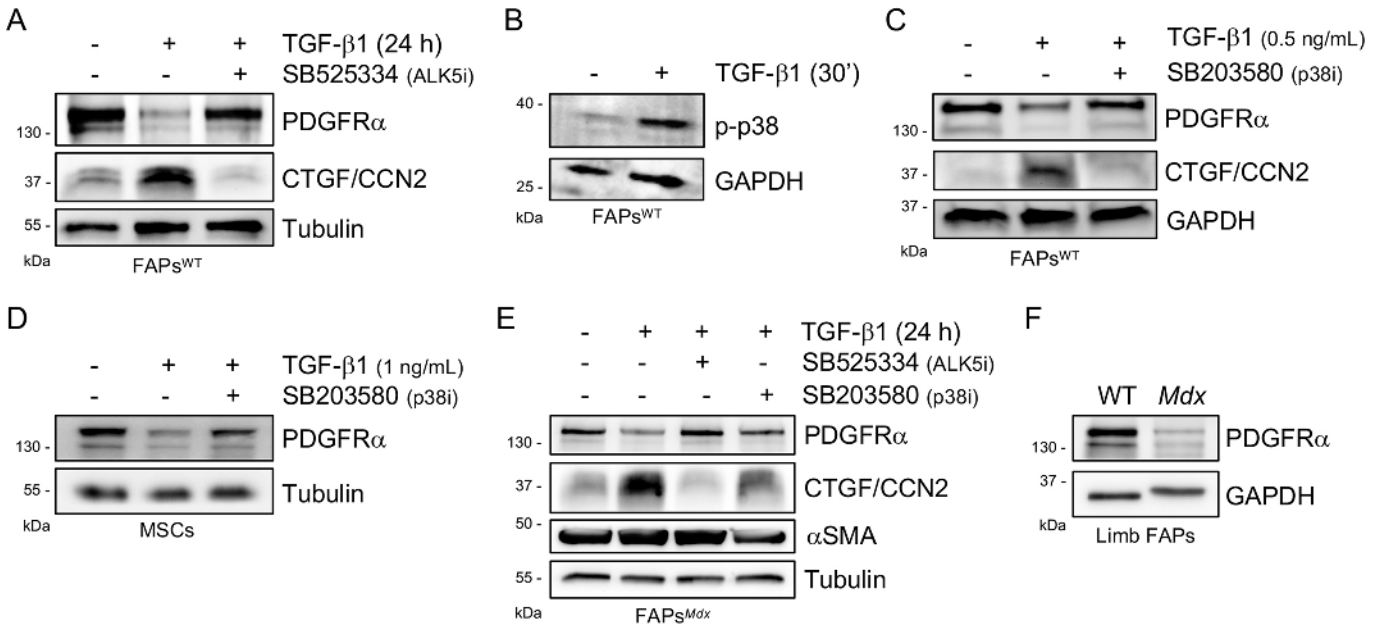

Fig. 4. TGF-β receptor type-I and p38 MAPK signaling participate in TGF-β-mediated PDGFRα downregulation. (A) Representative western blot analysis showing PDGFRα and CCN2 expression levels in wild-type FAPs after TGF-β1 treatment (5 ng/ml) for 24 h. SB525334 (TGFBR1 kinase inhibitor) was co-incubated with TGF-β1 for 24 h. Tubulin was used as the loading control. (B) Representative western blot showing p38 phosphorylation (p-p38) and GAPDH levels in wild-type FAPs after TGF-β1 stimulation for 30 min (30′). (C) Representative western blot analysis showing PDGFRα and CCN2 expression levels in wild-type FAPs after TGF-β1 treatment (0.5 ng/ml) for 24 h. SB203580 (p38 MAPK inhibitor) was co-incubated with TGF-β1 for 24 h. GAPDH was used as the loading control. (D) Representative western blot analysis showing PDGFRα expression levels in C3H 10T1/2 cells after TGF-β1 treatment (1 ng/ml) for 24 h. SB203580 (p38 MAPK inhibitor) was co-incubated with TGF-β1 for 24 h. Tubulin was used as the loading control. (E) Representative western blot analysis showing PDGFRα expression levels in *mdx* FAPs after TGF-β1 treatment (1 ng/ml) for 24 h. SB525334 (TGFBR1 kinase inhibitor) and SB203580 (p38 MAPK inhibitor) were co-incubated with TGF-β1. CCN2 and αSMA levels are also shown. Tubulin was used as the loading control. (F) Representative western blot analysis showing PDGFRα expression levels in wild-type and *mdx* cultured hindlimb FAPs.

IEG expression (Fig. 5B,C). SB525334 treatment strongly prevented *Txnip* reduction in response to TGF-β1 (Fig. 5C). Moreover, SB525334 abolished the increase in *Axud1* and *Schip1* expression triggered by TGF-β1 treatment (Fig. 5C). Interestingly, this TGFBR1 inhibitor also blocked TGF-β1-mediated effects on *Tiparp* and *Arid5b* expression (Fig. 5C). These results demonstrate that modulation of PDGFRα IEG expression in response to TGF-β requires the activity of TGF-β receptors. We also found a negative correlation between the fibrogenic activity of cardiac stromal fibroblast cells, and the expression of *Txnip* detected by scRNAseq (Fig. 5D). Hence, we have provided evidence that *Txnip* gene expression is repressed by TGF-β. Next, we asked whether TGF-β signaling regulates Txnip at the protein level. Txnip protein levels were downregulated in response to TGF-β1 in MSCs (Fig. 5E). Thus, TGF-β represses the expression of the PDGFRα target gene *Txnip* at the mRNA and protein levels.

PDGFRα signaling regulates TGF-β-mediated molecular and cellular responses

We have established that TGF-β activity regulates PDGFRα expression and signaling in the MSC lineage. Next, we explored whether PDGFRα activity plays a role in TGF-β-mediated effects on MSCs, and therefore, whether PDGFRα activity could participate in TGF-β1-induced myofibroblast differentiation, ECM remodeling and signaling. To examine this possibility, we used the PDGFRα/β kinase activity inhibitor AG1296 along with TGF-β in MSCs (Kovalenko et al., 1997). We observed that treatment with PDGFRα ligand PDGF-BB stimulates several PDGFR-dependent pathways such as AKT, ERK1/2, p38 and STAT3 (Fig. 6A,B), whereas treatment with AG1296 inhibited them (Fig. 6C). As a control, treatment with AG1296 alone did not interfere with the phosphorylation status of several downstream kinases of the PDGF and TGF-β pathways (Fig. S7A,B). Also, TGFBR1 kinase activity is not required for the PDGF-BB-dependent signaling cascade (Fig. 6C). Furthermore, inhibition of PDGFRα kinase activity with AG1296 blocked TGF-β1-induced expression of fibronectin, β1-integrin and CCN2 (Fig. 6D–F). Likewise, PDGFRα activity also participates in TGF-β-induced matrix remodeling of fibronectin (Fig. S8A–C). Mechanistically, we found that AG1296 inhibits TGF-β1-induced Smad2 phosphorylation (Fig. S8D). Moreover, TGF-β signaling seems not to affect PDGF-BB-dependent AKT and ERK activation (Fig. S8E). Finally, we also found that AG1296 partially inhibits the downregulation of PDGFRα and Txnip in response to TGF-β (Fig. 6G–I).

Additionally, AG1296 inhibits the phenotypic differentiation of MSCs into myofibroblasts induced by TGF-β1 (Fig. 7A,B). These results suggest that the pharmacological inhibition of PDGFRα influences TGF-β-triggered ECM remodeling, Smad2 phosphorylation and myofibroblast differentiation. Both TGF-β and PDGF signaling pathways are known regulators of mesenchymal cell migration and invasion (Hoch and Soriano, 2003; Mann et al., 2011). Since PDGFRα inhibition affects TGF-β-mediated molecular and cellular responses, we investigated whether inhibiting the kinase activity of PDGFRα impairs MSC cellular motility. The inhibition of PDGFRα by AG912 blocked the basal migration of MSCs in a scratch-wound assay (Fig. 7C,D). Furthermore, PDGFRα inhibition impaired TGF-β1-induced migration of mesenchymal cells (Fig. 7C,D). Taken together, these results suggest that PDGFRα is a critical regulator of the molecular, cellular and biological effects mediated by the TGF-β signaling pathway.

Journal of Cell Science (2019) 132, jcs232157. doi:10.1242/jcs.232157

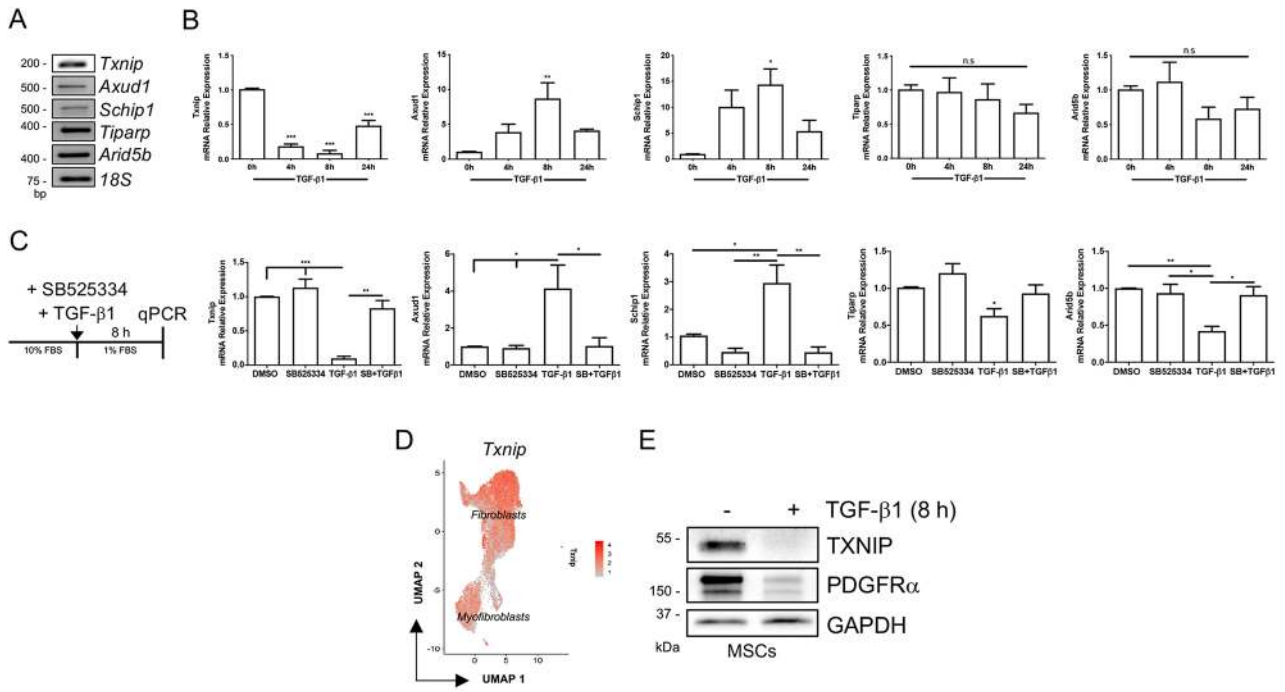

Fig. 5. TGF-β signaling alters the expression of PDGFRα-dependent immediate early genes. (A) RT-PCR analysis of *Txnip*, *Axud1*, *Schip1*, *Tiparp* and *Arid5b* expression in C3H/10T1/2 mesenchymal progenitors. The *18s* gene was used as a reference. bp, base pair. (B) *Txnip*, *Axud1*, *Schip1*, *Tiparp* and *Arid5b* mRNA expression levels were analyzed by quantitative PCR in C3H/10T1/2 mesenchymal progenitors after 4, 8 and 24 h of treatment with TGF-β1 (5 ng/ml). ***P<0.001; **P<0.005; *P<0.05; n.s., not significant by one-way ANOVA with Dunnett's post-test; n=3. (C) Treatment outline of cultured C3H 10T1/2 cells with TGF-β1 and SB525334. *Txnip*, *Axud1*, *Schip1*, *Tiparp* and *Arid5b* expression levels were analyzed by quantitative PCR in C3H/10T1/2 MSCs after 8 h treatment with TGF-β1 (5 ng/ml) and SB525334 (5 µM). ***P<0.001, **P<0.005, *P<0.05 by one-way ANOVA with Dunnett's post-test; n=3. (D) Single-cell RNA sequencing analyses showing the expression of *Txnip* in the cardiac stromal and fibroblast PDGFRα^{EGFP+} lineage using the UMAP algorithm. (E) Representative western blot analysis showing Txnip and PDGFRα protein levels in C3H/10T1/2 MSCs after 8 h treatment with TGF-β1 (5 ng/ml). GAPDH was used as the loading control.

DISCUSSION

Recent evidence suggests that adult tissue-resident mesenchyme populations are heterogeneous (Lemos and Duffield, 2018; Lynch and Watt, 2018). Central to this idea is that MSCs with different embryonic origins occupy particular niches and express unique molecular programs (Driskell et al., 2013; Malecova et al., 2018; Plikus et al., 2017; Rinkevich et al., 2015). Therefore, heterogeneous MSC populations and their lineage may have intrinsic properties that favor either permanent fibrosis or successful regeneration (Malecova et al., 2018; Rinkevich et al., 2015; Rognoni et al., 2018; Soliman et al., 2019 preprint) Furtado et al., 2016. Thus, investigating different sub-populations of stromal cells is important to understand how these cells and their fate influence regeneration and tissue repair.

Here, using a combination of several methodologies and analyses, we established that PDGFRα is a TGF-β target gene. First, we described that the number of FAPs correlates with TGF-β levels and with the degree of fibrosis in different models of skeletal muscle damage: glycerol, sciatic nerve denervation and muscular dystrophy. Second, we found that PDGFRα–EGFP$^{medium/low}$ cells expand from the PDGFRα^{+} population during skeletal muscle regeneration and repair. The PDGFRα–EGFP$^{medium/low}$ expression phenotype was associated with a more differentiated and fibrogenic cell state during MSC lineage progression following damage (Fig. 7E). Third, we showed that TGF-β signaling primes tissue-resident MSCs to become myofibroblasts instead of adipocytes, while downregulating PDGFRα expression in these cells (Fig. 7F). Finally, we suggest that PDGFRα plays a key role in TGF-β-mediated responses in MSCs, participating in TGF-β-regulated cellular and molecular responses, ECM remodeling and migration (Fig. 7G,H).

PDGFRα is an unequivocal marker for the identification of mesenchymal stromal cells in the embryo and the adult (Berry and Rodeheffer, 2013; Contreras et al., 2019; Malecova et al., 2018; Uezumi et al., 2014b; Vallecillo-García et al., 2017; Wosczyna and Rando, 2018; Furtado et al., 2016). Intriguingly, this RTK exhibits divergent roles in skeletal muscle. PDGFRα signaling is essential during mouse embryogenesis and muscle development (Hamilton et al., 2003; Schmahl et al., 2007; Soriano, 1997). PDGFRα also participates in ECM remodeling and angiogenesis during muscle growth and hypertrophy (Sugg et al., 2017). However, in adult skeletal muscle, increased PDGF ligand levels and enhanced PDGFRα pathway activity may cause pathological fibrosis (Ieronimakis et al., 2016; Uezumi et al., 2014a,b). Therefore, the PDGFRα pathway is a potential new target for the treatment of progressive degenerative pathologies where chronic damage and fibrosis are common factors (Contreras and Brandan, 2017; Smith and Barton, 2018).

PDGFRα has an essential and distinctive role in connective tissue remodeling (Horikawa et al., 2015). Besides, PDGFRα-activating mutations D842V and V561D, controlled by the endogenous *Pdgfra* promoter, lead to tissue fibrosis or connective tissue hyperplasia in several organs including muscle (Olson and Soriano, 2009). Transient PDGFRα activation in MSCs normally regulates repair of the injured muscle, but persistent and excessive activation of this pathway directly drives fibrosis by ECM-producing cells and hinders repair (Ieronimakis et al., 2016; Mueller et al., 2016). Interestingly,

Journal of Cell Science (2019) 132, jcs232157. doi:10.1242/jcs.232157

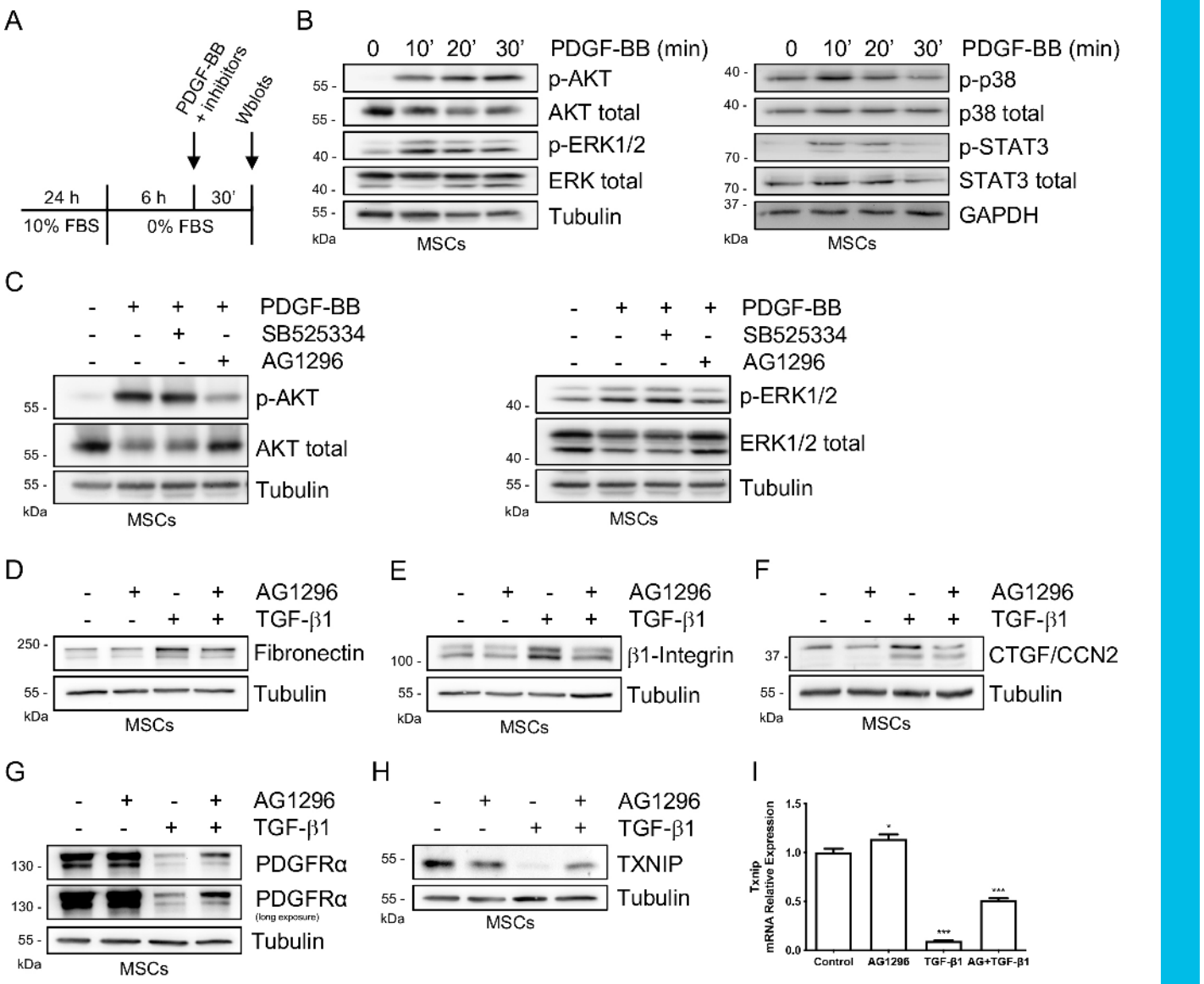

Fig. 6. PDGFRα participates in the molecular and cellular TGF-β-mediated responses. (A) Cell culture outline of PDGF-BB treatment of C3H 10T1/2 cells. (B) Representative time course western blot analysis showing total and phosphorylated levels of AKT, ERK1/2, p38 and STAT3 proteins after PDGF-BB treatment (20 ng/ml). Tubulin and GAPDH were used as loading controls. (C) Representative western blot analysis showing total and phosphorylated levels of AKT and ERK1/2 proteins after PDGF-BB (20 ng/ml), SB525334(5 µM) and AG1296 (10 µM) co-treatments. Tubulin was used as the loading control. (D–F) Representative western blot analysis from three independent experiments that evaluate total levels of fibronectin (D), β1-integrin (E) and CCN2 (F) following TGF-β1 (5 ng/ml) and AG1296 (10 µM) co-treatments. Tubulin was used as the loading control. (G,H) Representative western blot analysis from three independent experiments that evaluate total levels of PDGFRα (G) and Txnip (H) after TGF-β1 stimulation or AG1296 co-incubated with TGF-β1 for 24 h. Tubulin was used as the loading control. (I) *Txnip* mRNA expression was analyzed by quantitative PCR. ***P<0.001, *P<0.05 by one-way ANOVA with Dunnett's post-test; n=3.

the PDGFRα-activating mutation D842V in nestin^{+} cells causes white adipose tissue fibrosis in adult mice by converting adipogenic progenitor cells into ECM-producing fibroblasts, suggesting that PDGFRα has a pivotal role in fibroblast-adipocyte cell fate decisions (Iwayama et al., 2015). In support of this, another research group found, using a lineage-tracing approach, lipodystrophy and white adipose tissue fibrosis in young mice with the two different (V561D or D842V) PDGFRα-activating mutations mentioned above (Sun et al., 2017). Thus, these studies provide strong evidence that PDGFRα activity regulates the balance between adipocytes and stromal fibroblasts, which is crucial for proper adipose and connective tissue organogenesis and the development of fibrosis.

Two distinct types of interstitial tissue-resident lung fibroblasts have been identified through EGFP expression flow cytometry based in PDGFRα^{H2BEGFP} mice (Green et al., 2016). Another previous work has shown that the EGFP^{+} cell ratio (PDGFRα–EGFP^{high}/PDGFRα–EGFP^{medium}), and so the expression levels of PDGFRα, changed dynamically during lung regeneration (Chen et al., 2012). Recent and provocative work in injured heart demonstrated that PDGFRα–EGFP^{medium} cells identified in the heart after myocardial infarction are cardiac myofibroblasts. The authors observed a progressive accumulation of PDGFRα–EGFP^{medium} cells in the cardiac stromal lineage after MI and confirmed, using genetic lineage tracing experiments, that PDGFRα–EGFP^{high} cells give rise to the PDGFRα–EGFP^{medium} myofibroblasts (Asli et al., 2018 preprint). Here, PDGFRα$^{H2BEGFP/+}$ reporter mice helped us to discriminate different FAP sub-populations based on EGFP expression, but also to follow their behavior and fate during skeletal muscle repair. In

Journal of Cell Science (2019) 132, jcs232157. doi:10.1242/jcs.232157

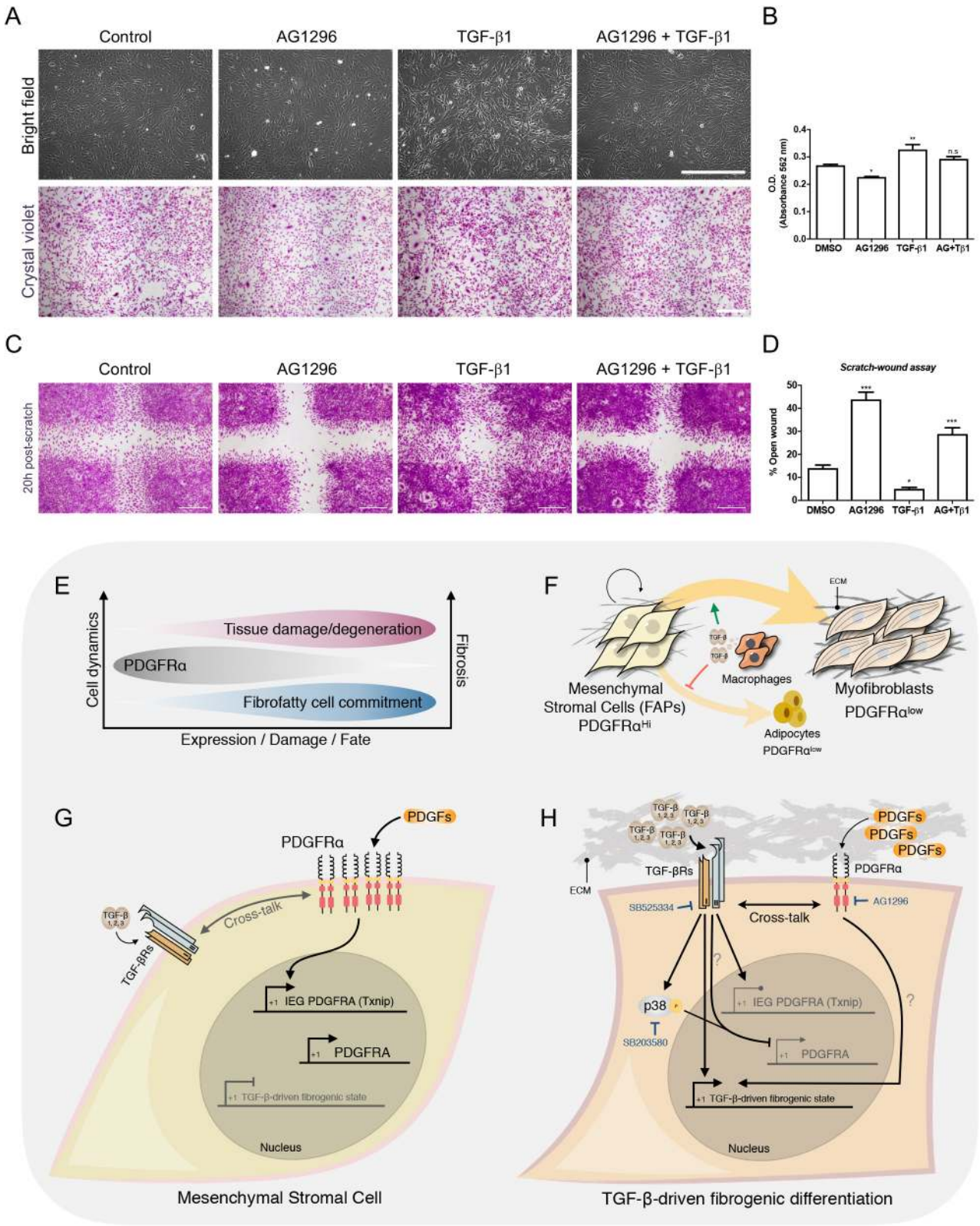

Fig. 7. See next page for legend.

undamaged muscle tissue the majority of naïve tissue-resident PDGFRα^{+} MSCs are PDGFRα–EGFP^{high} cells, consistent with previous studies demonstrating that most MSCs in uninjured tissues express PDGFRα at high levels (Asli et al., 2018 preprint; Kanisicak et al., 2016; Rognoni et al., 2018; Wosczyna and Rando, 2018), whereas PDGFRα–EGFP$^{medium/low}$ cells were highly enriched upon injury and identified as probably being myofibroblasts, as previously suggested (Tallquist and Molkentin, 2017). Taken together, these findings suggest that the expression of cell-type-specific markers varies during injury and is consistent with other recent lineage tracing

Fig. 7. PDGFRα modulates TGF-β-mediated biological responses. (A) Bright-field and Crystal Violet images showing that the inhibition of PDGFRα with AG1296 impairs TGF-β1-induced myofibroblast phenotype differentiation of C3H/10T1/2 MSCs after 24 h. (B) Total protein content in cells as shown in A was determined using a BCA assay kit, plotted as optical density (O.D.) obtained in control or treated cells. ***P*<0.005; **P*<0.05; n.s., not significant by one-way ANOVA with Dunnett's post-test; *n*=3. (C) Representative images of C3H/10T1/2 MSCs control-treated or treated with AG1296 and/or TGF-β1 for 20 h, and then stained with Crystal Violet following scratch-wound assay. (D) Quantification of the percentage of open wound area in cells as shown in C from three independent experiments. ****P*<0.001, **P*<0.05 by one-way ANOVA with Dunnett's post-test; *n*=3. Scale bars: 500 µm. (E–H) PDGFRα participation in stromal progenitors cell fate in response to tissue damage and TGF-β signaling. (E) Model of the relationship between PDGFRα expression in FAPs, tissue damage and fibrosis, and fibrofatty cell commitment. (F) TGF-β-driven myofibroblast differentiation impairs adipogenic commitment of stromal FAPs. MSCs and fibroblasts express high levels of PDGFRα in resting state, but low levels when differentiated and/or post-activation. (G,H) Upon tissue damage, TGF-β ligands released from macrophages and FAPs bind to TGF-β receptors (TGFBR1, TGFBR2 and TGFBR3) and activate TGFBR-dependent signaling cascades downregulating PDGFRα expression and impairing PDGFRα-dependent immediate early gene expression. Also, TGF-β-activated p38 MAPK negatively regulates PDGFRα. SB525334, SB203580 and AG1296 are TGFBR1, p38 MAPK, and PDGFRα kinase activity inhibitors, respectively.

studies (Kanisicak et al., 2016; Soliman et al., 2019 preprint; Tallquist and Molkentin, 2017).

Here, we linked PDGFRα with TGF-β signaling via the human BioGRID interactome and by analyzing the mouse PDGFRα promoter. Mechanistically, we demonstrated that non-canonical p38 MAPK signaling is activated by TGF-β and that both TGFBR1 and the p38 protein family participate in TGF-β-mediated downregulation of PDGFRα. We also described that several PDGFRα target genes are regulated in response to TGF-β in a TGFBR1-dependent manner. Concomitantly, PDGFRα IEG expression was altered in total tissue in these models. Using PDGFRα/β inhibitor AG1296, we found that PDGF-BB-stimulated PDGFRα signaling was essential to activate both proliferative and differentiation-related downstream signaling pathways such as ERK1/2, AKT, p38 and STAT3. PDGFRα signaling was also essential for the full TGF-β-driven differentiation of MSCs into myofibroblasts and ECM remodeling, probably involving activation of the TGF-β-activated canonical Smad2/3 signaling pathway.

FAP proliferation and survival depend on a complex balance of tumor necrosis factor-alpha (TNF-α) and TGF-β produced by a different set of inflammatory cells (Lemos et al., 2015). TNF-α induces FAP apoptosis. However, TGF-β promotes both FAP proliferation and survival *in vivo* and *in vitro* (Contreras et al., 2019; Lemos et al., 2015; Uezumi et al., 2011). In addition, TGF-β induces the differentiation of murine and human FAPs into myofibroblasts rather than adipocytes (Uezumi et al., 2014a, 2011), which supports our results. Conversely, PDGF-AA stimulation of FAPs upregulates several matrix proteins and induces downstream ERK1/2 and AKT PDGFRα and Smad2/3 TGF-β signaling pathways (Mueller et al., 2016; Uezumi et al., 2014a). These results and our work suggest that the cross-talk between PDGFRα and TGF-β signaling pathways regulates FAP activation and fate, but also suggest that MSC activation and differentiation could be linked to proliferation. It has been shown that PDGF-AB promotes activation and proliferation of injury-activated $EGFP^{+}$ stromal cardiac fibroblasts, but does not influence PDGFRα–$EGFP^{medium}$ myofibroblasts (Asli et al., 2018 preprint). Because PDGFRα downregulation is a hallmark of myofibroblasts in the context of injury, we hypothesize that the impact of PDGF ligands on the MSC lineage relates to a predominant role in naïve or undifferentiated PDGFRα–$EGFP^{high}$ mesenchymal stromal cells rather than PDGFRα–$EGFP^{medium/low}$ differentiated cells. Thus, cellular PDGFRα bioavailability may be a determinant factor in PDGF-dependent responses of MSCs during fate decisions and injury-related behaviors.

Others have proposed that PDGFRα regulates, via differential transcriptional and posttranscriptional regulation of TGF-β receptors, TGF-β-driven activation of hepatic stellate cells (Liu et al., 2014). Contrary to the results presented here, it has been shown that TGF-β upregulates PDGFRα in hepatocytes, scleroderma fibroblasts and tumor cells (Gotzmann et al., 2006; Leof et al., 1986; Yamakage et al., 1992). Nevertheless, TGF-β downregulates PDGFRα expression in human lung fibroblasts and smooth muscle cells (Battegay et al., 1990; Bonner et al., 1995). It has been suggested that myostatin (MSTN), another TGF-β family member, along with inducing FAP proliferation and differentiation into myofibroblasts, leads to decreased PDGFRα expression (Dong et al., 2017). Here, we present data supporting that the injury-induced fibrogenic milieu reduced PDGFRα expression in FAPs and MSCs, and therefore, we propose the model shown in Fig. 7E–H. Furthermore, TGF-β signaling regulates the expression of several IEGs of the PDGF pathway, unveiling a previously undetected cross-talk between TGF-β and PDGF signaling. Among the PDGFRα target genes, *Txnip*, which was also generally repressed in our different models of muscle damage and in response to TGF-β, emerges as an interesting new TGF-β target gene candidate for further study. In mouse embryonic fibroblasts, Txnip is suppressed by the activation of PDGFRα (Wu et al., 2008). However, TGF-β1 upregulates Txnip in tumor cells and during cell cycle arrest (Han et al., 2003). In addition, Txnip is typically silenced in cancer cells, hence its tumor suppression function has emerged as an interesting target in cancer biology (Alhawiti et al., 2017). In summary, we suggest that TGF-β signaling has a regulatory role in PDGFRα expression and function that in progenitor cells could be acting as negative profibrotic feedback. We hypothesized that TGF-β release in the stromal space after injury primes the tissue-resident MSCs to differentiate toward non-expressing PDGFRα myofibroblasts, which then are unresponsive to the self-renewal PDGF signaling. This makes sense in a context in which it is important to restrain an exacerbated stromal response to control the tissue fibrotic response by stromal cells. Thus, PDGFRα and TGF-β signaling could interact in a cell-specific and complex arrangement during regeneration. Hence, the results presented here reveal a novel concept where TGF-β and PDGFRα interplay in the control of progenitor cell fate, signaling, ECM remodeling and migration.

IL-4 signaling has been shown to serve as a key switch to control FAP biology (Heredia et al., 2013). During acute damage, activation of IL-4 signaling induces FAP proliferation to support myogenesis, while preventing FAPs from undergoing adipogenic differentiation (Heredia et al., 2013). The function of interleukins or TNF-α signaling on PDGFRα expression has not been addressed yet, which indicates that complete and more in-depth research about other signals regulating FAP behavior is needed. In the last few years, we have gained knowledge of the roles of TGF-β and PDGFRα in myopathies and fibrosis (Ceco and McNally, 2013; Smith and Barton, 2018). Here, we hypothesize that PDGFRα could work in modulating fibrogenesis and connective tissue remodeling in conjunction with TGF-β during scar formation and regression. On top of that, further combined and multi-targeting therapies are needed for both key FAP modulators. The tyrosine kinase inhibitor nilotinib, restores FAP apoptosis by blocking TGF-β-triggered p38 kinase activation (Lemos et al., 2015). Nilotinib also inhibits PDGFRα and p38, along with other tyrosine kinases (Contreras

et al., 2018). Accordingly, SB431542, a potent and specific inhibitor of transforming growth factor-β superfamily type I receptors [ALK4 (also known as ACVR1B), TGFBR1 and ALK7 (also known as ACVR1C)], promotes FAP apoptosis in injured rotator cuff muscle (Davies et al., 2016). Consequently, it is necessary to look for new approaches to target FAPs and their signaling pathways to develop effective therapeutic strategies for preventing pathological changes following injury and disease.

The study of stromal MSC biology and their fine-tuned regulation may hold the key for augmenting muscle regeneration, since ablation of FAPs causes impaired muscle regeneration (Fiore et al., 2016; Mueller et al., 2016; Murphy et al., 2011; Wosczyna et al., 2019). Future studies should focus on elucidating the diverse differentiation mechanisms governing FAP fate. The identification of genes and molecules that regulate FAP activity to promote myogenic regeneration without fibrotic and fatty tissue deposition is likely to offer great therapeutic benefits for the aging population, and for neuromuscular diseases, and severely injured skeletal muscle.

MATERIALS AND METHODS

Mice and study approval

Housing, husbandry and experimental protocols were conducted in strict accordance and with the formal approval of the Animal Ethics Committee of the Pontificia Universidad Católica de Chile (Doctoral ID protocol: 160512005) and following institutional and national guidelines at the University of British Columbia, Canada. Mice were housed in standard cages under 12-h light-dark cycles and fed *ad libitum* with a standard chow diet. Five-month-old C57BL/10ScScJ male mice (hereafter referred to as wild type, WT; stock #000476) and dystrophic C57BL/10ScSn-*Dmd*^{mdx}/J mice (stock #001801) male mice (both from Jackson Laboratories) were used in experiments for Fig. S1M. For PDGFRα IEG expression in WT and *mdx* mice, we used 24-month-old mice. *Pdgfra*$^{tm11(EGFP)Sor}$ mice (hereafter referred to as PDGFRα^{H2BEGFP} mice) were purchased from Jackson Laboratories (stock #007669 B6.129S4-Pdgfra$^{tm11(EGFP)Sor}$/J; Hamilton et al., 2003). Because of the protein stability of H2B-EGFP, it can be helpful as a short-term *in vivo* lineage tag. For FAP detection in *mdx* muscles, we crossed male C57Bl/10ScSn-mdx mice with hemizygous female B6.129S4-Pdgfra$^{tm11(EGFP)Sor}$/J mice. We used the F1 male *mdx*;PDGFRα^{H2BEGFP} offspring (5- to 6-month-old), and the comparisons were performed among siblings. All surgeries were performed after the mice had been anesthetized with 2.5–3% of isoflurane gas in pure oxygen. The mice were euthanized with cervical dislocation at the ages indicated in each figure, and the tissues were immediately processed, either by direct freezing in liquid nitrogen for protein and RNA extraction or in 2-methyl butane cooled with liquid nitrogen for histological analysis as described below.

Skeletal muscle injury and denervation

For acute glycerol injury, the tibialis anterior (TA) muscle of 2- to 3-month-old PDGFRα^{H2BEGFP} mice was injected with 50 µl 50% v/v glycerol. Tissue collection was performed as indicated in the corresponding figures after glycerol injections. Notexin muscle damage was induced by intramuscular injection of 0.15 µg notexin snake venom (Latoxan) into the TA muscle (Joe et al., 2010; Lemos et al., 2015). Non-injected muscles from the contralateral limb were used as a control. Sciatic nerve denervation was performed unilaterally in 5-month-old WT and PDGFRα^{H2BEGFP} mice as described previously (Contreras et al., 2016). Denervated mice were euthanized 4 days or 2 weeks after denervation, and the gastrocnemius muscles from the contralateral and denervated hind limbs were collected (Rebolledo et al., 2019). The contralateral muscles of the non-denervated limb were used as controls. For fibrotic-*mdx* muscle experiments, *mdx* mice (*mdx*;PDGFRα^{H2BEGFP}) were used at 8–10 weeks of age and TA muscle was experimentally microinjured over 2 weeks to induce chronic tissue damage and the establishment of fibrosis after 1 week of rest (fibrotic-*mdx* TA; Desguerre et al., 2012). Muscles were isolated and collected for analysis at the time points indicated in the figures.

Tissue preparation, flow cytometry and FACS

One-step digestion of tissue for FAPs was performed mainly as described before with some modifications (Judson et al., 2017; Lemos et al., 2015). All the steps were performed on ice unless otherwise specified. Briefly, skeletal muscle from both hindlimbs (limb FAPs), and diaphragm (diaphragm FAPs) was carefully dissected, washed with 1×PBS, cut into small pieces with scissors until homogeneous. Collagenase D (Roche Biochemicals) 1.5 U/ml and Dispase II (Roche Biochemicals) 2.4 U/ml, in 2.5 mM $CaCl_2$, was added to every two hindlimbs in a total volume of 3 ml per mouse, and the preparation was placed at 37°C for 45 min with rotation. Preparations were passed through a 70 µm, and then 40 µm cell strainer (Becton Dickenson), and washed with FACS buffer (PBS, 2% FBS, 2 mM EDTA pH 7.9). Resulting single cells were collected by centrifugation at 1000 ***g*** for 5–10 min. Cell preparations were incubated with primary antibodies for 20–30 min at 4°C in FACS buffer at ∼3×10^7 cells/ml. We used the following monoclonal primary antibodies: anti-CD31 (clones MEC13.3, Cat. no. 553372, Becton Dickenson; clone 390, Cat. no. CL8930F-3, 1:500, Cedarlane Laboratories), anti-CD45 (clone 30-F11, Cat. no. 557659, 1:400, Becton Dickenson), anti-CD45.1 (1:400; clone A20, Cat. no. 553775, 1:400, Becton Dickenson), anti-CD45.2 (clone 104, Cat. no. 11-0454-85, eBiosciences), anti-Sca-1 (1:2000–1:5000; clone D7, Cat. no. 25-5981-82, Invitrogen) and anti-α7 integrin (1:11500; Clone R2F2, Cat. no. 67-0010-05, AbLab). For all antibodies, we performed fluorescence minus one control by staining with appropriate isotype control antibodies (rat IgG2a kappa, PE-Cyanine7, clone eBR2a, Cat. no. 25-4321-82, eBioscience. 1:400; mouse anti-IgG2a k, FITC, clone G155-178, BD, Cat No: 553456; rat IgG2b kappa, APC, clone eB149/10H5, Cat. no. 17-4031-82 – all from eBioscience). To assess viability, cells were stained with propidium iodide (1 µg ml^{-1}) and Hoechst 33342 (2.5 µg ml^{-1}) and resuspended at ∼1×10^6 cells ml^{-1} immediately before sorting or analysis. The analysis was performed on a LSRII (Becton Dickenson) flow cytometer equipped with three lasers. Data were collected using FacsDIVA software. Cell sorting was performed on a FACS Vantage SE (Becton Dickenson), BD Influx flow cytometer (Becton Dickinson), or FACS Aria (Becton Dickenson), all equipped with three lasers, using a 100-µm nozzle at 18 psi to minimize the effects of pressure on the cells. Sorting gates were strictly defined based on isotype control (fluorescence minus one) stains. Cd140a (PDGFRA) flow cytometry analysis (using rat anti-mouse CD140a APC, clone APA5, Cat. no. 17-1401-81, eBiosciences at 1:200) was performed in C3H/10T1/2 cells on a BD Influx flow cytometer (Becton Dickinson) using 561 nm excitation laser. All flow cytometry data were analyzed using FlowJo 10.5.3v.

Reagents

The tyrphostin PDGFRα/β inhibitor AG1296 (mostly used at 10 µM final concentration; ab141170, Abcam), TGFBR1 inhibitor SB525334 (used at 5 µM; S8822, Sigma-Aldrich), p38 MAPK SB203580 inhibitor (used at 20 µM; 5633, Cell Signaling Technology), PI3K/AKT inhibitor LY294002 (used at 10 µM; 440202, Merck-Calbiochem), the inhibitor of MEK1/2/ERK1/2 kinases UO126 (used at 10 µM; 9903, Cell Signaling Technology), and the inhibitor of JNK activity SB600125 (used at 20 µM; Cell Signaling Technology) were all diluted in DMSO. DMSO alone was used as a control. Cycloheximide (C104450, Sigma-Aldrich) was diluted in ethanol and used at 30µg/ml final concentration. All the inhibitors used were added at the same time and co-incubated with TGF-β1.

Cell culture

The murine mesenchymal stromal cell (MSC) cell line C3H/10T1/2, Clone 8, and the embryonic fibroblast cell line NIH-3T3 were obtained from American Type Culture Collection (ATCC) and grown at 37°C in 5% CO_2 in growth medium (GM): high-glucose Dulbecco's modified Eagle's medium (DMEM) (Invitrogen) with 10% fetal bovine serum (FBS; Hyclone) and supplemented with antibiotics (Gutiérrez et al., 2015). Mouse dermal fibroblasts (MDFs) were obtained from the skin as previously described (Gutiérrez et al., 2015). Cells were treated with recombinant human TGF-β1 (580702, BioLegend), recombinant human TGF-β2 (583301, BioLegend, USA), recombinant human TGF-β3 (501123524, eBioscience) in DMEM supplemented with 2% (v/v) FBS and penicillin/streptomycin in a 5% CO_2 atmosphere at

concentration and time indicated in the corresponding figure legend. For phosphorylation studies, cells were serum-starved as indicated in the figures. Adipogenic differentiation of C3H/10T1/2 MSCs was induced for 14–21 days with MesenCult Adipogenic Differentiation Kit (Mouse) according to the manufacturer's instructions (STEMCELL Technologies). Our cell cultures were periodically tested to ensure no mycoplasma contamination using polymerase chain reaction (PCR).

FAPs cell culture

FAPs were FACS sorted from either wild-type or PDGFRα$^{H2BEGFP/+}$ mice and grown in high-glucose DMEM (Invitrogen), supplemented with 10% FBS, 1% sodium pyruvate, and 2.5 ng/ml bFGF (Invitrogen) at a density of 15,000 cell/cm^2 in a 48-well plate or 24-well plate. Cells were isolated from undamaged muscles. For the TGF-β1 treatment experiment, after 72 h in culture and 70–80% confluence, FAPs were stimulated with 5 ng/ml TGF-β1. Cells were then collected for further analyses. Adipogenic differentiation of FAPs was induced for 10–14 days with MesenCult Adipogenic Differentiation Kit (Mouse) according to the manufacturer's instructions.

Protein extraction and western blot analyses

Protein extracts from cells were obtained using RIPA 1× lysis buffer (9806, Cell Signaling Technology) plus protease or phosphatase inhibitors (P8340 or P0044, Sigma-Aldrich). The cells were sonicated for 10 s and centrifuged at 9000 ***g***. Proteins were quantified using a Micro BCA assay kit, following the manufacturer's instructions (Pierce). Extracts were subjected to SDS-PAGE electrophoresis in 9–10% polyacrylamide gels, transferred to PVDF membranes (Millipore), and probed with primary antibodies: goat anti-PDGFRα (1:1000; AF1062, R&D Systems), mouse anti-alpha smooth muscle actin (αSMA) (1:1000; A5228, Sigma-Aldrich), rabbit anti-perilipin A/B (1:200; P1873, Sigma-Aldrich), goat anti-CCN2 (1:500; Cat. no. sc-14939, Santa Cruz Biotechnology), rabbit anti-integrin β1 (M-106) (1:1000; sc-8978, Santa Cruz Biotechnology), rabbit anti-fibronectin (1:2000; F3648, Sigma-Aldrich), mouse anti-VDUP1 (Txnip) (D-2) (1:1000; sc-271237, Santa Cruz Biotechnology), mouse anti-GAPDH (1:5000; MAB374, Millipore), mouse anti-α-tubulin (1:5000; T5168, Sigma-Aldrich), rabbit anti-phospho-p44/42 MAPK (ERK1/2) (1:1000; 9101S, Cell Signaling Technology), rabbit anti-p44/42 MAPK (ERK1/2) (1:1000; 9102, Cell Signaling Technology), rabbit anti-phospho-AKT (ser473) (1:1000; 9271S, Cell Signaling Technology), rabbit anti-AKT (1:1000; 9272, Cell Signaling Technology), rabbit anti-phospho p38 (Thr180/Tyr182) (1:500; 9211S, Cell Signaling Technology), rabbit anti-p38 (1:1000; 9212, Cell Signaling Technology), rabbit anti-phospho-SAPK/JNK (1:1000; Thr183/Tyr185; 9251, Cell Signaling Technology), rabbit anti-TGFBR1 (1:500; ab31013, Abcam), mouse anti-TGF-BR2 (C-4) (1:500; sc-17791, Santa Cruz Biotechnology), goat anti-TGFBR3 (1:1000; ab18885, Abcam), rabbit anti-Smad2 phospho-specific (Ser465/467) (1:1000; AB3849 Chemicon, Merck Millipore), rabbit anti-phospho-Stat3 (Tyr705) (1:2000; 9131, Cell Signaling Technology), mouse-anti Stat3 (F-2) (1:1000; sc-8019, Santa Cruz Biotechnology). Then, primary antibodies were detected with a secondary antibody conjugated to horseradish peroxidase: mouse anti-goat IgG (1:5000; 31400), goat anti-rabbit IgG (1:5000; 31460) and goat anti-mouse IgG (1:5000; 31430), all from Pierce. All immunoreactions were visualized by enhanced chemiluminescence Super Signal West Dura (34075, Pierce) or Super Signal West Femto (34096, Pierce) by a ChemiDoc-It HR 410 imaging system (UVP). Western blot densitometry quantification was done using Fiji software (ImageJ version 2.0.0-rc/69/1.52n). Protein levels were normalized with the levels of the loading control. Ponceau S Red Staining Solution [0.1% (w/v) in 5% (v/v) acetic acid] was used. The blots that are shown in Fig. 3N,B, Fig. S3B and Fig. S4C,H were subsequently incubated with secondary antibodies labeled with IRDye 800 and IRDye 680 (1:10.000–1:20.000, Cat. nos 926-32214 and 926-68070, respectively, LI-COR Biosciences). Signal was detected using a Li-Cor Odyssey scanner (LI-COR Biosciences).

Indirect immunofluorescence and microscopy

For immunofluorescence, flash-frozen muscles were transversally sectioned at 7 µm, fixed for 15 min in 4% paraformaldehyde, and washed in phosphate-buffered saline (PBS). Tissue sections were blocked for 30–60 min in 1% bovine serum albumin (BSA) plus 1% fish gelatin in PBS, incubated overnight at 4°C in primary antibodies: rabbit anti-collagen I (1:250; A34710, Abcam), goat anti-PDGFRα (1:100; AF1062, R&D Systems), rabbit anti-fibronectin (1:200; F3648; Sigma-Aldrich). Samples were then washed in PBS, incubated for 1 h at room temperature with a secondary antibody (Alexa-Fluor-488 chicken anti-goat IgG (H+L), Cat. no. A21467, Invitrogen; Alexa-Fluor-568 donkey anti-rabbit IgG (H+L), Cat. no. A10042, Life Technologies; Alexa-Fluor-594 donkey anti-rabbit IgG (H+L), Cat. no. A21207, Life Technologies; Alexa-Fluor-488 goat anti-rabbit IgG (H+L), 1:500, Cat. no. A11008, Life Technologies; Alexa-Fluor-555 donkey anti-mouse IgG (H+L), Cat. no. A31570, Invitrogen; all used at 1:500) and washed in PBS. Hoechst 33342 stain (2 mg/ml) and wheat germ agglutinin (WGA) Alexa-Fluor-594 conjugate (1:250; W11262, Invitrogen) were added for 10 min diluted in PBS before the slides were mounted, according to the manufacturer's instructions. To stain F-actin, Alexa-Fluor-568 phalloidin was added to the cells according to the manufacturer's instructions (1:50; A12380, ThermoFisher) for 10 min along with Hoechst 33342 stain. Slides were then washed in abundant PBS and mounted with fluorescent mounting medium (DAKO). Cells were imaged on a Nikon Eclipse C2 Si Confocal Spectral Microscope or Nikon Eclipse Ti Confocal Microscope using Nikon NIS-Elements AR software 4.00.00 (build 764) LO, 64 bit. Confocal images were acquired at the Unidad de Microscopía Avanzada (UMA), Pontificia Universidad Católica de Chile, using a Nikon Eclipse C2 Si confocal spectral microscope. Plan-Apochromat objectives were used (Nikon, VC 20× DIC N2 NA 0.75, 40× OIL DIC H NA 1.0, and, VC 60× OIL DIC NA 1.4). Fluorescence microscopy images shown in Fig. S1A,E,I were acquired with an Nikon Eclipse E600 epifluorescence microscope. Confocal microscopy images shown in Fig. 1A were composed using maximum-intensity projection *z*-stack reconstructions (0.3 µm each stack) of 7-µm-thick transversal sections. Then, we manually analyzed the percentage of PDGFRα–EGFP$^{medium/low}$-expressing FAPs in regeneration and repair using the cell counter plugging from Fiji software (ImageJ version 2.0.0-rc/69/1.52n, NIH). Counts of 4–8 randomly chosen fields and mild and severe damage fields were averaged from four independent experiments.

RNA isolation, reverse transcription and quantitative real-time polymerase chain reaction

Total RNA from cultured cells was isolated using TRIzol (Invitrogen) according to the manufacturer's instructions. RNA integrity was corroborated as described previously (Contreras et al., 2018). 2 µg of RNA was reverse transcribed into cDNA using random primers and M-MLV reverse transcriptase (Invitrogen). Quantitative real-time polymerase chain reaction (RT-qPCR) was performed in triplicate with the Eco Real-Time PCR System (Illumina), using primer sets for *Txnip*, *Tiparp*, *Axud1*, *Arid5b*, *Schip1*, *Pparg*, *Adipoq*. and the housekeeping gene *18s* (used as a reference gene). The ΔΔCt method was used for quantification, and mRNA levels were expressed relative to the mean levels of the control condition in each case. We analyzed and validated each RT-qPCR expected gene product using a 2% agarose gel. Primers used are listed in Table S2.

Bioinformatics analysis with single-cell RNA-seq data

For single-cell RNA sequencing, data graphical output, merging, subsetting and quality control of datasets were performed via Seurat R package (Satija Lab, v.3.02) where ggplot2 was used to draw the graphs in Fig. 1E (Butler et al., 2018) by using the Uniform Manifold Approximation and Projection (UMAP) algorithm (McInnes et al., 2018). Scatter plots depicting Pearson's correlation between the normalized counts of *Tgfb* (*Tgfb1,2,3*) versus *Pdgfra* or *Pdgfra*^{EGFP} in Fig. S2 were produced using the ggscatter() function from the ggpubr package (https://github.com/kassambara/ggpubr). The correlation analyses were generated from the RNA sequencing dataset, GFP_ShamVsMI_days3_7, available in the ArrayExpress database at EMBL-EBI1072 (www.ebi.ac.uk/arrayexpress) under accession codes E-MTAB-7376 and E-MTAB-7365 (Farbehi et al., 2019). While Fig. S2A includes all cells, Fig. S2B only includes cells that express at least one count of Periostin (Postn).

Computational BioGRID database, PDGFRα promoter analysis and Tabula Muris open source database

The image in Fig. S3A was generated with BioGRID based on human PDGFRA (Stark, 2006). The data from figures and tables in the BioGRID webpage (https://thebiogrid.org/) can be searched and sorted. For the promoter analysis of mouse PDGFRα shown in Table 1, we used MatInspector software following the supplier's instructions (https://www.genomatix.de). The Murine Tabula Muris database was used to generate the figures shown in Fig. S2B,C (The Tabula Muris Consortium et al., 2018). Data were extracted and analyzed from limb muscles.

Scratch-wound assay

The scratch-wound assay was performed as previously described with few modifications (Liang et al., 2007). In brief, C3H/10T1/2 mesenchymal progenitors were cultured (20,000 cells/cm^2) in growth medium for 24 h until 90–100% confluence. Then, the cell medium was changed to 1% FBS and the cells were treated with TGF-β1 (5 ng/ml) and AG1296 (10 µM) for 20 h. Sterile p200 pipet tips were used to perform the scratch wound. DMSO was used as the control. At the end of the experiment, the cells were washed with 1×PBS and stained with Crystal Violet staining solution (0.5% w/v) (C3886, Sigma-Aldrich) as described previously (Contreras et al., 2018). Stained cells were imaged with a Nikon Eclipse N600 microscope. We measured the total scratch-wounded area and the area not covered by cells in six randomly chosen fields in three independent experiments. Quantification was done using Fiji software (ImageJ version 2.0.0-rc/69/1.52n, NIH).

Statistical analysis

Mean±s.e.m. values, as well as the number of experiments performed, are indicated in each figure. All data sets were analyzed for normal distribution using the D'agostino normality test. Statistical significance of the differences between the means was evaluated using the one-way analysis of variance test (ANOVA) followed by post-hoc Dunnett's multiple comparison test and the significance level set at $P \leq 0.05$. A two-tailed Student's *t*-test was performed when two conditions were compared. Differences were considered significant with $P \leq 0.05$. Data were collected in Microsoft Excel, and statistical analyses were performed using Prism 8 software for macOS (GraphPad).

Acknowledgements

We are grateful to the Unidad de Microscopía Avanzada (UMA) of Pontificia Universidad Católica de Chile for its support in image acquisition. We acknowledge the services provided by the UC CINBIOT Animal Facility funded by the PIA CONICYT* ECM-07 Program for Associative Research, of the Chilean National Council for Science and Technology. We thank the animal unit staff and Ms Micaela Ricca of Pontificia Universidad Católica de Chile. We also acknowledge the animal unit staff and genotyping core facility at the Biomedical Research Centre, especially Mr Taka Murakami, Mrs Krista Ranta and Mr Wei Yuan. We thank Mr Andy Johnson and Mr Justin Wong of UBC Flow Cytometry. We are grateful to Ms Alicia Minniti for proofreading the article. We acknowledge the Larrain Lab (Pontificia Universidad Católica de Chile) and the Mario Chiong Lab (Universidad de Chile) for providing STAT3 antibodies and PDGF-BB ligand, respectively. For administrative assistance, we thank Ms Vanessa Morales and Ms Vittoria Canale. We also acknowledge Eduardo Ramirez, Darling Vera and Bastián Marquez for their technical support.

Competing interests

The authors declare no competing or financial interests.

Author contributions

Conceptualization: O.C., E.B.; Methodology: O.C., M.C.-S., M.T., H.S., L.W.T.; Software: O.C., H.S., L.W.T., E.G.; Validation: O.C., M.C.-S., M.T., H.S., L.W.T., E.G., F.M.R., E.B.; Formal analysis: O.C., M.C.-S., E.B.; Investigation: O.C., M.C.-S., M.T., H.S., L.W.T., F.M.R.; Resources: O.C., F.M.R., E.B.; Data curation: O.C., M.C.-S., E.B.; Writing - original draft: O.C.; Writing - review & editing: O.C., M.T., H.S., E.G., F.M.R., E.B.; Visualization: O.C., M.C.-S., M.T., H.S., L.W.T., F.M.R., E.B.; Supervision: O.C., F.M.R., E.B.; Project administration: O.C., E.B.; Funding acquisition: O.C., E.B., F.M.R.

Funding

Fondo Nacional de Desarrollo Científico y Tecnológico (FONDECYT) grant 1190144 and Comisión Nacional de Investigación Científica y Tecnológica (CONICYT) grant AFB170005 to E.B.; CONICYT Beca de Doctorado Nacional Folio 21140378 to O.C.; CONICYT Beca de Doctorado Nacional Folio 21170735 to M.C.-S.; and Canadian Institutes of Health Research (CIHR) grant FDN-159908 to F.M.R. supported this work. The funding agencies had no role in the design of the study, data collection, analysis, the decision to publish or preparation of the manuscript.

Supplementary information

Supplementary information available online at
http://jcs.biologists.org/lookup/doi/10.1242/jcs.232157.supplemental

References

Accornero, F., Kanisicak, O., Tjondrokoesoemo, A., Attia, A. C., McNally, E. M. and Molkentin, J. D. (2014). Myofiber-specific inhibition of TGFβ signaling protects skeletal muscle from injury and dystrophic disease in mice. *Hum. Mol. Genet.* **23**, 6903-6915. doi:10.1093/hmg/ddu413

Acuña, M. J., Pessina, P., Olguin, H., Cabrera, D., Vio, C. P., Bader, M., Muñoz-Canoves, P., Santos, R. A., Cabello-Verrugio, C. and Brandan, E. (2014). Restoration of muscle strength in dystrophic muscle by angiotensin-1-7 through inhibition of TGF-β signalling. *Hum. Mol. Genet.* **23**, 1237-1249. doi:10.1093/hmg/ddt514

Alhawiti, N. M., Al Mahri, S., Aziz, M. A., Malik, S. S. and Mohammad, S. (2017). TXNIP in metabolic regulation: physiological role and therapeutic outlook. *Curr. Drug Targets.* **18**, 1095-1103. doi:10.2174/1389450118666170130145514

Asli, N. S., Xaymardan, M., Patrick, R., Farbehi, N., Cornwell, J., Forte, E., Waardenberg, A. J., Janbandhu, V., Kesteven, S., Chandrakanthan, V., et al. (2018). PDGFRα signaling in cardiac fibroblasts modulates quiescence, metabolism and self-renewal, and promotes anatomical and functional repair. *BioRxiv*, 225979. doi:10.1101/225979

Battegay, E. J., Raines, E. W., Seifert, R. A., Bowen-Pope, D. F. and Ross, R. (1990). TGF-β induces bimodal proliferation of connective tissue cells via complex control of an autocrine PDGF loop. *Cell* **63**, 515-524. doi:10.1016/0092-8674(90)90448-N

Bernasconi, P., Di Blasi, C., Mora, M., Morandi, L., Galbiati, S., Confalonieri, P., Cornelio, F. and Mantegazza, R. (1999). Transforming growth factor-β1 and fibrosis in congenital muscular dystrophies. *Neuromuscul. Disord.* **9**, 28-33. doi:10.1016/S0960-8966(98)00093-5

Berry, R. and Rodeheffer, M. S. (2013). Characterization of the adipocyte cellular lineage in vivo. *Nat. Cell Biol.* **15**, 302. doi:10.1038/ncb2696

Bonner, J. C., Badgett, A., Lindroos, P. M. and Osornio-Vargas, A. R. (1995). Transforming growth factor beta 1 downregulates the platelet-derived growth factor alpha-receptor subtype on human lung fibroblasts in vitro. *Am. J. Respir. Cell Mol. Biol.* **13**, 496-505. doi:10.1165/ajrcmb.13.4.7546780

Braun, T., Buschhausen-Denker, G., Bober, E., Tannich, E. and Arnold, H. H. (1989). A novel human muscle factor related to but distinct from MyoD1 induces myogenic conversion in 10T1/2 fibroblasts. *EMBO J.* **8**, 701-709. doi:10.1002/j.1460-2075.1989.tb03429.x

Butler, A., Hoffman, P., Smibert, P., Papalexi, E. and Satija, R. (2018). Integrating single-cell transcriptomic data across different conditions, technologies, and species. *Nat. Biotechnol.* **36**, 411-420. doi:10.1038/nbt.4096

Callahan, J. F., Burgess, J. L., Fornwald, J. A., Gaster, L. M., Harling, J. D., Harrington, F. P., Heer, J., Kwon, C., Lehr, R., Mathur, A. et al. (2002). Identification of novel inhibitors of the transforming growth factor β1 (TGF- β1) type 1 receptor (ALK5). *J. Med. Chem.* **45**, 999-1001. doi:10.1021/jm010493y

Ceco, E. and McNally, E. M. (2013). Modifying muscular dystrophy through transforming growth factor-β. *FEBS J.* **280**, 4198-4209. doi:10.1111/febs.12266

Chen, W. V., Delrow, J., Corrin, P. D., Frazier, J. P. and Soriano, P. (2004). Identification and validation of PDGF transcriptional targets by microarray-coupled gene-trap mutagenesis. *Nat. Genet.* **36**, 304-312. doi:10.1038/ng1306

Chen, L., Acciani, T., Le Cras, T., Lutzko, C. and Perl, A.-K. T. (2012). Dynamic regulation of platelet-derived growth factor receptor alpha expression in alveolar fibroblasts during realveolarization. *Am. J. Respir. Cell Mol. Biol.* **47**, 517-527. doi:10.1165/rcmb.2012-0030OC

Cohn, R. D., van Erp, C., Habashi, J. P., Soleimani, A. A., Klein, E. C., Lisi, M. T., Gamradt, M., ap Rhys, C. M., Holm, T. M., Loeys, B. L. et al. (2007). Angiotensin II type 1 receptor blockade attenuates TGF-β-induced failure of muscle regeneration in multiple myopathic states. *Nat. Med.* **13**, 204-210. doi:10.1038/nm1536

Contreras, O. and Brandan, E. (2017). Fibro/adipogenic progenitors safeguard themselves: a novel mechanism to reduce fibrosis is discovered. *J. Cell Commun. Signal.* **11**, 77-78. doi:10.1007/s12079-016-0372-4

Contreras, O., Rebolledo, D. L., Oyarzún, J. E., Olguín, H. C. and Brandan, E. (2016). Connective tissue cells expressing fibro/adipogenic progenitor markers increase under chronic damage: relevance in fibroblast-myofibroblast differentiation and skeletal muscle fibrosis. *Cell Tissue Res.* **364**, 647-660. doi:10.1007/s00441-015-2343-0

Contreras, O., Villarreal, M. and Brandan, E. (2018). Nilotinib impairs skeletal myogenesis by increasing myoblast proliferation. *Skelet Muscle* **8**, 5. doi:10.1186/s13395-018-0150-5

Contreras, O., Rossi, F. M. and Brandan, E. (2019). Adherent muscle connective tissue fibroblasts are phenotypically and biochemically equivalent to stromal fibro/adipogenic progenitors. *Matrix Biol. Plus* **2**, 100006. doi:10.1016/J.MBPLUS.2019.04.003

D'Addario, M., Arora, P. D., Ellen, R. P. and McCulloch, C. A. G. (2002). Interaction of p38 and Sp1 in a mechanical force-induced, beta 1 integrin-mediated transcriptional circuit that regulates the actin-binding protein filamin-A. *J. Biol. Chem.* **277**, 47541-47550. doi:10.1074/jbc.M207681200

Danna, N. R., Beutel, B. G., Campbell, K. A. and Bosco, J. A.III. (2014). Therapeutic approaches to skeletal muscle repair and healing. *Sports Health.* **6**, 348-355. doi:10.1177/1941738113512261

David, C. J. and Massagué, J. (2018). Contextual determinants of TGFβ action in development, immunity and cancer. *Nat. Rev. Mol. Cell Biol.* **19**, 419-435. doi:10.1038/s41580-018-0007-0

Davies, M. R., Liu, X., Lee, L., Laron, D., Ning, A. Y., Kim, H. T. and Feeley, B. T. (2016). TGF-β small molecule inhibitor SB431542 reduces rotator cuff muscle fibrosis and fatty infiltration by promoting fibro/adipogenic progenitor apoptosis. *PLoS ONE* **11**, e0155486. doi:10.1371/journal.pone.0155486

Derynck, R. and Zhang, Y. E. (2003). Smad-dependent and Smad-independent pathways in TGF-β family signalling. *Nature* **425**, 577-584. doi:10.1038/nature02006

Desguerre, I., Arnold, L., Vignaud, A., Cuvellier, S., Yacoub-Youssef, H., Gherardi, R. K., Chelly, J., Chretien, F., Mounier, R., Ferry, A. et al. (2012). A new model of experimental fibrosis in hindlimb skeletal muscle of adult mdx mouse mimicking muscular dystrophy. *Muscle Nerve* **45**, 803-814. doi:10.1002/mus.23341

Dong, J., Dong, Y., Chen, Z., Mitch, W. E. and Zhang, L. (2017). The pathway to muscle fibrosis depends on myostatin stimulating the differentiation of fibro/adipogenic progenitor cells in chronic kidney disease. *Kidney Int.* **91**, 119-128. doi:10.1016/j.kint.2016.07.029

Driskell, R. R., Lichtenberger, B. M., Hoste, E., Kretzschmar, K., Simons, B. D., Charalambous, M., Ferron, S. R., Herault, Y., Pavlovic, G., Ferguson-Smith, A. C. et al. (2013). Distinct fibroblast lineages determine dermal architecture in skin development and repair. *Nature* **504**, 277-281. doi:10.1038/nature12783

Farbehi, N., Patrick, R., Dorison, A., Xaymardan, M., Janbandhu, V., Wystub-Lis, K., Ho, J. W. K., Nordon, R. E. and Harvey, R. P. (2019). Single-cell expression profiling reveals dynamic flux of cardiac stromal, vascular and immune cells in health and injury. *eLife* **8**, e43882. doi:10.7554/eLife.43882

Fiore, D., Judson, R. N., Low, M., Lee, S., Zhang, E., Hopkins, C., Xu, P., Lenzi, A., Rossi, F. M. V. and Lemos, D. R. (2016). Pharmacological blockage of fibro/adipogenic progenitor expansion and suppression of regenerative fibrogenesis is associated with impaired skeletal muscle regeneration. *Stem Cell Res.* **17**, 161-169. doi:10.1016/j.scr.2016.06.007

Furtado, M. B., Nim, H. T., Boyd, S. E. and Rosenthal, N. A. (2016). View from the heart: cardiac fibroblasts in development, scarring and regeneration. *Development* **143**, 387-397. doi:10.1242/dev.120576

Gonzalez, D., Contreras, O., Rebolledo, D. L., Espinoza, J. P., van Zundert, B. and Brandan, E. (2017). ALS skeletal muscle shows enhanced TGF-β signaling, fibrosis and induction of fibro/adipogenic progenitor markers. *PLoS ONE* **12**, e0177649. doi:10.1371/journal.pone.0177649

Gosselin, L. E., Williams, J. E., Deering, M., Brazeau, D., Koury, S. and Martinez, D. A. (2004). Localization and early time course of TGF-β1 mRNA expression in dystrophic muscle. *Muscle Nerve* **30**, 645-653. doi:10.1002/mus.20150

Gotzmann, J., Fischer, A. N. M., Zojer, M., Mikula, M., Proell, V., Huber, H., Jechlinger, M., Waerner, T., Weith, A., Beug, H. et al. (2006). A crucial function of PDGF in TGF-β-mediated cancer progression of hepatocytes. *Oncogene* **25**, 3170-3185. doi:10.1038/sj.onc.1209083

Green, J., Endale, M., Auer, H. and Perl, A.-K. T. (2016). Diversity of interstitial lung fibroblasts is regulated by platelet-derived growth factor receptor α kinase activity. *Am. J. Respir. Cell Mol. Biol.* **54**, 532-545. doi:10.1165/rcmb.2015-0095OC

Gutiérrez, J., Droppelmann, C. A., Contreras, O., Takahashi, C. and Brandan, E. (2015). RECK-mediated β1-integrin regulation by TGF-β1 is critical for wound contraction in mice. *PLoS ONE* **10**, e0135005. doi:10.1371/journal.pone.0135005

Hamilton, T. G., Klinghoffer, R. A., Corrin, P. D. and Soriano, P. (2003). Evolutionary divergence of platelet-derived growth factor alpha receptor signaling mechanisms. *Mol. Cell. Biol.* **23**, 4013-4025. doi:10.1128/MCB.23.11.4013-4025.2003

Han, S. H., Jeon, J. H., Ju, H. R., Jung, U., Kim, K. Y., Yoo, H. S., Lee, Y. H., Song, K. S., Hwang, H. M., Na, Y. S. et al. (2003). VDUP1 upregulated by TGF-β1 and 1,25-dihydorxyvitamin D3 inhibits tumor cell growth by blocking cell-cycle progression. *Oncogene* **22**, 4035-4046. doi:10.1038/sj.onc.1206610

Heredia, J. E., Mukundan, L., Chen, F. M., Mueller, A. A., Deo, R. C., Locksley, R. M., Rando, T. A. and Chawla, A. (2013). Type 2 innate signals stimulate fibro/adipogenic progenitors to facilitate muscle regeneration. *Cell* **153**, 376-388. doi:10.1016/j.cell.2013.02.053

Hinz, B., Phan, S. H., Thannickal, V. J., Galli, A., Bochaton-Piallat, M.-L. and Gabbiani, G. (2007). The myofibroblast: one function, multiple origins. *Am. J. Pathol.* **170**, 1807-1816. doi:10.2353/ajpath.2007.070112

Hoch, R. V. and Soriano, P. (2003). Roles of PDGF in animal development. *Development* **130**, 4769-4784. doi:10.1242/dev.00721

Horikawa, S., Ishii, Y., Hamashima, T., Yamamoto, S., Mori, H., Fujimori, T., Shen, J., Inoue, R., Nishizono, H., Itoh, H. et al. (2015). PDGFRα plays a crucial role in connective tissue remodeling. *Sci. Rep.* **5**, 17948. doi:10.1038/srep17948

Ieronimakis, N., Hays, A., Prasad, A., Janebodin, K., Duffield, J. S. and Reyes, M. (2016). PDGFRα signalling promotes fibrogenic responses in collagen-producing cells in Duchenne muscular dystrophy. *J. Pathol.* **240**, 410-424. doi:10.1002/path.4801

Iwayama, T., Steele, C., Yao, L., Dozmorov, M. G., Karamichos, D., Wren, J. D. and Olson, L. E. (2015). PDGFRα signaling drives adipose tissue fibrosis by targeting progenitor cell plasticity. *Genes Dev.* **29**, 1106-1119. doi:10.1101/gad.260554.115

Joe, A. W. B., Yi, L., Natarajan, A., Le Grand, F., So, L., Wang, J., Rudnicki, M. A. and Rossi, F. M. V. (2010). Muscle injury activates resident fibro/adipogenic progenitors that facilitate myogenesis. *Nat. Cell Biol.* **12**, 153-163. doi:10.1038/ncb2015

Juban, G., Saclier, M., Yacoub-Youssef, H., Kernou, A., Arnold, L., Boisson, C., Ben Larbi, S., Magnan, M., Cuvellier, S., Théret, M. et al. (2018). AMPK activation regulates LTBP4-dependent TGF-β1 secretion by pro-inflammatory macrophages and controls fibrosis in Duchenne muscular dystrophy. *Cell Rep.* **25**, 2163-2176.e6. doi:10.1016/j.celrep.2018.10.077

Judson, R. N., Low, M., Eisner, C. and Rossi, F. M. (2017). Isolation, culture, and differentiation of fibro/adipogenic progenitors (FAPs) from skeletal muscle. *Methods Mol. Biol.* **1668**, 93-103. doi:10.1007/978-1-4939-7283-8_7

Kanisicak, O., Khalil, H., Ivey, M. J., Karch, J., Maliken, B. D., Correll, R. N., Brody, M. J., J. Lin, S.-C., Aronow, B. J., Tallquist, M. D. et al. (2016). Genetic lineage tracing defines myofibroblast origin and function in the injured heart. *Nat. Commun.* **7**, 12260. doi:10.1038/ncomms12260

Kim, K. K., Sheppard, D. and Chapman, H. A. (2018). TGF-β1 signaling and tissue fibrosis. *Cold Spring Harb. Perspect. Biol.* **10**, a022293. doi:10.1101/cshperspect.a022293

Kopinke, D., Roberson, E. C. and Reiter, J. F. (2017). Ciliary Hedgehog signaling restricts injury-induced adipogenesis. *Cell* **170**, 340-351.e12. doi:10.1016/j.cell.2017.06.035

Kovalenko, M., Rönnstrand, L., Heldin, C.-H., Loubtchenkov, M., Gazit, A., Levitzki, A. and Böhmer, F. D. (1997). Phosphorylation site-specific inhibition of platelet-derived growth factor β-receptor autophosphorylation by the receptor blocking tyrphostin AG1296. *Biochemistry* **36**, 6260-6269. doi:10.1021/bi962553l

Laping, N. J., Everitt, J. I., Frazier, K. S., Burgert, M., Portis, M. J., Cadacio, C., Gold, L. I. and Walker, C. L. (2007). Tumor-specific efficacy of transforming growth factor-βRI inhibition in Eker rats. *Clin. Cancer Res.* **13**, 3087-3099. doi:10.1158/1078-0432.CCR-06-1811

Lemos, D. R., Babaeijandaghi, F., Low, M., Chang, C.-K., Lee, S. T., Fiore, D., Zhang, R.-H., Natarajan, A., Nedospasov, S. A. and Rossi, F. M. V. (2015). Nilotinib reduces muscle fibrosis in chronic muscle injury by promoting TNF-mediated apoptosis of fibro/adipogenic progenitors. *Nat. Med.* **21**, 786-794. doi:10.1038/nm.3869

Lemos, D. R. and Duffield, J. S. (2018). Tissue-resident mesenchymal stromal cells: Implications for tissue-specific antifibrotic therapies. *Science Translational Medicine*. doi:10.1126/scitranslmed.aan5174

Leof, E. B., Proper, J. A., Goustin, A. S., Shipley, G. D., DiCorleto, P. E. and Moses, H. L. (1986). Induction of c-sis mRNA and activity similar to platelet-derived growth factor by transforming growth factor beta: a proposed model for indirect mitogenesis involving autocrine activity. *Proc. Natl. Acad. Sci. USA* **83**, 2453-2457. doi:10.1073/pnas.83.8.2453

Lepper, C., Partridge, T. A. and Fan, C.-M. (2011). An absolute requirement for Pax7-positive satellite cells in acute injury-induced skeletal muscle regeneration. *Development* **138**, 3639-3646. doi:10.1242/dev.067595

Liang, C.-C., Park, A. Y. and Guan, J.-L. (2007). In vitro scratch assay: a convenient and inexpensive method for analysis of cell migration in vitro. *Nat. Protoc.* **2**, 329-333. doi:10.1038/nprot.2007.30

Liu, C., Guo, L., Tu, K., Kang, N., Shah, V. H., Xiang, X., Liu, Q. and Li, J. (2014). PDGF receptor-α promotes TGF-β signaling in hepatic stellate cells via transcriptional and posttranscriptional regulation of TGF-β receptors. *Am. J. Physiol. Gastrointest. Liver Physiol.* **307**, G749-G759. doi:10.1152/ajpgi.00138.2014

Lukjanenko, L., Brachat, S., Pierrel, E., Lach-Trifilieff, E. and Feige, J. N. (2013). Genomic profiling reveals that transient adipogenic activation is a hallmark of mouse models of skeletal muscle regeneration. *PLoS ONE* **8**, e71084. doi:10.1371/journal.pone.0071084

Lynch, M. D. and Watt, F. M. (2018). Fibroblast heterogeneity: implications for human disease. *J. Clin. Investig.* **128**, 26-35. doi:10.1172/JCI93555

McInnes, L. and Healy, J. (2018). UMAP: Uniform Manifold Approximation and Projection for Dimension Reduction, arXiv:1802.03426v2.

Ma, W., Lim, W., Gee, K., Aucoin, S., Nandan, D., Kozlowski, M., Diaz-Mitoma, F. and Kumar, A. (2001). The p38 mitogen-activated kinase pathway regulates the human interleukin-10 promoter via the activation of Sp1 transcription factor in lipopolysaccharide-stimulated human macrophages. *J. Biol. Chem.* **276**, 13664-13674. doi:10.1074/jbc.M011157200

Madaro, L., Passafaro, M., Sala, D., Etxaniz, U., Lugarini, F., Proietti, D., Alfonsi, M. V., Nicoletti, C., Gatto, S., De Bardi, M. et al. (2018). Denervation-activated STAT3–IL-6 signalling in fibro-adipogenic progenitors promotes myofibres atrophy and fibrosis. *Nat. Cell Biol.* **20**, 917-927. doi:10.1038/s41556-018-0151-y

Malecova, B., Gatto, S., Etxaniz, U., Passafaro, M., Cortez, A., Nicoletti, C., Giordani, L., Torcinaro, A., De Bardi, M., Bicciato, S. et al. (2018). Dynamics of cellular states of fibro-adipogenic progenitors during myogenesis and muscular dystrophy. *Nat. Commun.* **9**, 3670. doi:10.1038/s41467-018-06068-6

Mann, C. J., Perdiguero, E., Kharraz, Y., Aguilar, S., Pessina, P., Serrano, A. L. and Muñoz-Cánoves, P. (2011). Aberrant repair and fibrosis development in skeletal muscle. *Skelet. Muscle* **1**, 21. doi:10.1186/2044-5040-1-21

Marinkovic, M., Fuoco, C., Sacco, F., Cerquone Perpetuini, A., Giuliani, G., Micarelli, E., Pavlidou, T., Petrilli, L. L., Reggio, A., Riccio, F. et al. (2019). Fibro-adipogenic progenitors of dystrophic mice are insensitive to NOTCH regulation of adipogenesis. *Life Sci. Alliance* **2**, e201900437. doi:10.26508/lsa.201900437

Mathew, S. J., Hansen, J. M., Merrell, A. J., Murphy, M. M., Lawson, J. A., Hutcheson, D. A., Hansen, M. S., Angus-Hill, M. and Kardon, G. (2011). Connective tissue fibroblasts and Tcf4 regulate myogenesis. *Development* **138**, 371-384. doi:10.1242/dev.057463

Mueller, A. A., van Velthoven, C. T., Fukumoto, K. D., Cheung, T. H. and Rando, T. A. (2016). Intronic polyadenylation of PDGFRα in resident stem cells attenuates muscle fibrosis. *Nature* **540**, 276-279. doi:10.1038/nature20160

Murphy, M. M., Lawson, J. A., Mathew, S. J., Hutcheson, D. A. and Kardon, G. (2011). Satellite cells, connective tissue fibroblasts and their interactions are crucial for muscle regeneration. *Development* **138**, 3625-3637. doi:10.1242/dev.064162

Olson, L. E. and Soriano, P. (2009). Increased PDGFRα activation disrupts connective tissue development and drives systemic fibrosis. *Dev. Cell* **16**, 303-313. doi:10.1016/j.devcel.2008.12.003

Pessina, P., Kharraz, Y., Jardí, M., Fukada, S., Serrano, A. L., Perdiguero, E. and Muñoz-Cánoves, P. (2015). Fibrogenic cell plasticity blunts tissue regeneration and aggravates muscular dystrophy. *Stem Cell Rep.* **4**, 1046-1060. doi:10.1016/j.stemcr.2015.04.007

Plikus, M. V., Guerrero-Juarez, C. F., Ito, M., Li, Y. R., Dedhia, P. H., Zheng, Y., Shao, M., Gay, D. L., Ramos, R., Hsi, T.-C. et al. (2017). Regeneration of fat cells from myofibroblasts during wound healing. *Science* **355**, 748-752. doi:10.1126/science.aai8792

Rebolledo, D. L., González, D., Faundez-Contreras, J., Contreras, O., Murphy-Ullrich, J. E., Lipson, K. E. and Brandan, E. (2019). Denervation-induced skeletal muscle fibrosis is mediated by CTGF/CCN2 independently of TGF-β. *Matrix Biol.* **82**, 20-37. doi:10.1016/J.MATBIO.2019.01.002

Reznikoff, C. A., Bertram, J. S., Brankow, D. W. and Heidelberger, C. (1973). Quantitative and qualitative studies of chemical transformation of cloned C3H mouse embryo cells sensitive to postconfluence inhibition of cell division. *Cancer Res.* **33**, 3239-3249.

Rinkevich, Y., Walmsley, G. G., Hu, M. S., Maan, Z. N., Newman, A. M., Drukker, M., Januszyk, M., Krampitz, G. W., Gurtner, G. C., Lorenz, H. P. et al. (2015). Identification and isolation of a dermal lineage with intrinsic fibrogenic potential. *Science* **348**, aaa2151. doi:10.1126/science.aaa2151

Riquelme-Guzmán, C., Contreras, O. and Brandan, E. (2018). Expression of CTGF/CCN2 in response to LPA is stimulated by fibrotic extracellular matrix via the integrin/FAK axis. *Am. J. Physiol. Cell Physiol.* **314**, C415-C427. doi:10.1152/ajpcell.00013.2017

Rognoni, E., Pisco, A. O., Hiratsuka, T., Sipilä, K. H., Belmonte, J. M., Mobasseri, S. A., Philippeos, C., Dilão, R. and Watt, F. M. (2018). Fibroblast state switching orchestrates dermal maturation and wound healing. *Mol. Syst. Biol.* **14**, e8174. doi:10.15252/msb.20178174

Sambasivan, R., Yao, R., Kissenpfennig, A., Van Wittenberghe, L., Paldi, A., Gayraud-Morel, B., Guenou, H., Malissen, B., Tajbakhsh, S. and Galy, A. (2011). Pax7-expressing satellite cells are indispensable for adult skeletal muscle regeneration. *Development* **138**, 3647-3656. doi:10.1242/dev.067587

Schmahl, J., Raymond, C. S. and Soriano, P. (2007). PDGF signaling specificity is mediated through multiple immediate early genes. *Nat. Genet.* **39**, 52-60. doi:10.1038/ng1922

Singh, R., Artaza, J. N., Taylor, W. E., Gonzalez-Cadavid, N. F. and Bhasin, S. (2003). Androgens stimulate myogenic differentiation and inhibit adipogenesis in C3H 10T1/2 pluripotent cells through an androgen receptor-mediated pathway. *Endocrinology* **144**, 5081-5088. doi:10.1210/en.2003-0741

Smith, L. R. and Barton, E. R. (2018). Regulation of fibrosis in muscular dystrophy. *Matrix Biol.* **68-69**, 602-615. doi:10.1016/j.matbio.2018.01.014

Soliman, H., Paylor, B., Scott, W., Lemos, D., Chang, C. K., Arostegui, M., Low, M., Lee, C., Fiore, D., Braghetta, P., et al. (2019). Pathogenic potential of Hic1 expressing cardiac stromal progenitors. *BioRxiv*, 544403. doi:10.1101/544403

Soriano, P. (1997). The PDGF alpha receptor is required for neural crest cell development and for normal patterning of the somites. *Development.* **124**, 2691-2700.

Stark, C. (2006). BioGRID: a general repository for interaction datasets. *Nucleic Acids Research*. doi:10.1093/nar/gkj109

Sugg, K. B., Korn, M. A., Sarver, D. C., Markworth, J. F. and Mendias, C. L. (2017). Inhibition of platelet-derived growth factor signaling prevents muscle fiber growth during skeletal muscle hypertrophy. *FEBS Lett.* **591**, 801-809. doi:10.1002/1873-3468.12571

Sun, C., Berry, W. L. and Olson, L. E. (2017). PDGFRα controls the balance of stromal and adipogenic cells during adipose tissue organogenesis. *Development.* **144**, 83-94. doi:10.1242/dev.135962

Tallquist, M. D. and Molkentin, J. D. (2017). Redefining the identity of cardiac fibroblasts. *Nature Reviews Cardiology,* **14**, 484. doi:10.1038/nrcardio.2017.57

The Tabula Muris Consortium, **Overall coordination**, **Logistical coordination**, **Organ collection and processing; Library preparation and sequencing**, **Computational data analysis**, **Cell type annotation**, **Writing group**, **Supplemental text writing group** and **Principal investigators**. (2018). Single-cell transcriptomics of 20 mouse organs creates a Tabula Muris. *Nature* **562**, 367-372. doi:10.1038/s41586-018-0590-4

Uezumi, A., Fukada, S.-I., Yamamoto, N., Takeda, S. and Tsuchida, K. (2010). Mesenchymal progenitors distinct from satellite cells contribute to ectopic fat cell formation in skeletal muscle. *Nat. Cell Biol.* **12**, 143-152. doi:10.1038/ncb2014

Uezumi, A., Ito, T., Morikawa, D., Shimizu, N., Yoneda, T., Segawa, M., Yamaguchi, M., Ogawa, R., Matev, M. M., Miyagoe-Suzuki, Y. et al. (2011). Fibrosis and adipogenesis originate from a common mesenchymal progenitor in skeletal muscle. *J. Cell Sci.* **124**, 3654-3664. doi:10.1242/jcs.086629

Uezumi, A., Fukada, S., Yamamoto, N., Ikemoto-Uezumi, M., Nakatani, M., Morita, M., Yamaguchi, A., Yamada, H., Nishino, I., Hamada, Y. et al. (2014a). Identification and characterization of PDGFRα+ mesenchymal progenitors in human skeletal muscle. *Cell Death Dis.* **5**, e1186. doi:10.1038/cddis.2014.161

Uezumi, A., Ikemoto-Uezumi, M. and Tsuchida, K. (2014b). Roles of nonmyogenic mesenchymal progenitors in pathogenesis and regeneration of skeletal muscle. *Front Physiol.* **5**, 68. doi:10.3389/fphys.2014.00068

Vallecillo-García, P., Orgeur, M., Vom Hofe-Schneider, S., Stumm, J., Kappert, V., Ibrahim, D. M., Börno, S. T., Hayashi, S., Relaix, F., Hildebrandt, K. et al. (2017). Odd skipped-related 1 identifies a population of embryonic fibro-adipogenic progenitors regulating myogenesis during limb development. *Nat. Commun.* **8**, 1218. doi:10.1038/s41467-017-01120-3

Vidal, B., Serrano, A. L., Tjwa, M., Suelves, M., Ardite, E., De Mori, R., Baeza-Raja, B., Martínez de Lagrán, M., Lafuste, P., Ruiz-Bonilla, V. et al. (2008). Fibrinogen drives dystrophic muscle fibrosis via a TGFβ/alternative macrophage activation pathway. *Genes Dev.* **22**, 1747-1752. doi:10.1101/gad.465908

Wosczyna, M. N. and Rando, T. A. (2018). A muscle stem cell support group: coordinated cellular responses in muscle regeneration. *Dev. Cell.* **46**, 135-143. doi:10.1016/j.devcel.2018.06.018

Wosczyna, M. N., Biswas, A. A., Cogswell, C. A. and Goldhamer, D. J. (2012). Multipotent progenitors resident in the skeletal muscle interstitium exhibit robust BMP-dependent osteogenic activity and mediate heterotopic ossification. *J. Bone Miner. Res.* **27**, 1004-1017. doi:10.1002/jbmr.1562

Wosczyna, M. N., Konishi, C. T., Perez Carbajal, E. E., Wang, T. T., Walsh, R. A., Gan, Q., Wagner, M. W. and Rando, T. A. (2019). Mesenchymal stromal cells are required for regeneration and homeostatic maintenance of skeletal muscle. *Cell Rep.* **27**, 2029-2035.e5. doi:10.1016/j.celrep.2019.04.074

Wu, E., Palmer, N., Tian, Z., Moseman, A. P., Galdzicki, M., Wang, X., Berger, B., Zhang, H. and Kohane, I. S. (2008). Comprehensive dissection of PDGF-PDGFR signaling pathways in PDGFR genetically defined cells. *PLoS ONE* **3**, e3794. doi:10.1371/journal.pone.0003794

Yamakage, A., Kikuchi, K., Smith, E. A., LeRoy, E. C. and Trojanowska, M. (1992). Selective upregulation of platelet-derived growth factor α receptors by transforming growth factor β in scleroderma fibroblasts. *J. Exp. Med.* **175**, 1227-1234. doi:10.1084/jem.175.5.1227

Zhang, Y. E. (2017). Non-Smad signaling pathways of the TGF-β family. *Cold Spring Harbor Perspect. Biol.* **9**, a022129. doi:10.1101/cshperspect.a022129